

Escaping Saddle Points with Stochastically Controlled Stochastic Gradient Methods

Guannan Liang

GUANNAN.LIANG@UCONN.EDU

Qianqian Tong

QIANQIAN.TONG@UCONN.EDU

Chunjiang Zhu

CHUNJIANG.ZHU@UCONN.EDU

Jinbo Bi

JINBO.BI@UCONN.EDU

*University of Connecticut
Storrs, CT 06269, USA*

Editor:

Abstract

Stochastically controlled stochastic gradient (SCSG) methods have been proved to converge efficiently to first-order stationary points which, however, can be saddle points in nonconvex optimization. It has been observed that a stochastic gradient descent (SGD) step introduces anisotropic noise around saddle points for deep learning and non-convex half space learning problems, which indicates that SGD satisfies the correlated negative curvature (CNC) condition for these problems. Therefore, we propose to use a separate SGD step to help the SCSG method escape from strict saddle points, resulting in the CNC-SCSG method. The SGD step plays a role similar to noise injection but is more stable. We prove that the resultant algorithm converges to a second-order stationary point with a convergence rate of $\tilde{O}(\epsilon^{-2} \log(1/\epsilon))$ where ϵ is the pre-specified error tolerance. This convergence rate is independent of the problem dimension, and is faster than that of CNC-SGD. A more general framework is further designed to incorporate the proposed CNC-SCSG into any first-order method for the method to escape saddle points. Simulation studies illustrate that the proposed algorithm can escape saddle points in much fewer epochs than the gradient descent methods perturbed by either noise injection or a SGD step.

Keywords: nonconvex optimization, SCSG methods, escaping saddle points

1. Introduction

In this paper, the problem of interest is the nonconvex finite-sum problem of the form

$$\min_{x \in \mathbb{R}^d} f(x) := \frac{1}{n} \sum_{z=1}^n f_z(x), \tag{1}$$

where both f and f_z ($z \in [n] := \{1, 2, \dots, n\}$) may be nonconvex, and their gradients and Hessians are Lipschitz continuous. Problem (1) plays an essential role in many machine learning methods especially in the training of deep neural networks. The stochastic gradient descent (SGD) method and its variants are commonly used for solving (1). However, finding global or local minimum of f generally is NP-hard (Anandkumar and Ge, 2016). Hence, people turn to find sub-optimal solutions for Problem (1), such as first-order stationary points (Nesterov, 2013) or second-order stationary points (Ge et al., 2015).

An ϵ -first-order stationary point x can be guaranteed by the gradient descent (GD) method and its variants, such that for an arbitrarily small $\epsilon > 0$,

$$\|\nabla f(x)\| \leq \epsilon \quad (2)$$

(Nesterov, 2013; Ghadimi, 2016; Carmon et al., 2017; Reddi et al., 2016; Lei et al., 2017). Specifically, for a smooth nonconvex f , an ϵ -first-order stationary point can be found by the GD in $\mathcal{O}(\epsilon^{-2})$ iterations, or by the SGD in $\mathcal{O}(\epsilon^{-4})$ iterations (Nesterov, 2013) where ϵ is the error tolerance chosen beforehand. Later, the accelerated gradient descent (AGD) method also achieved a convergence rate $\mathcal{O}(\epsilon^{-2})$ (Ghadimi, 2016), and the Guarded-AGD algorithm improved over the AGD algorithm and reached a convergence rate $\mathcal{O}(\epsilon^{-\frac{7}{4}})$. However, ϵ -first-order stationary points can be saddle points or even local maximizers in non-convex optimization (Jin et al., 2017).

Hence, there has been theoretical analysis to find second-order stationary points for Problem (1) (Ge et al., 2015; Jin et al., 2017; Nesterov, 2006) where an (ϵ_g, ϵ_h) -second-order stationary point x is sought such that:

$$\|\nabla f(x)\| \leq \epsilon_g \quad \text{and} \quad \nabla^2 f(x) \succeq -\epsilon_h I \quad (3)$$

for some small positive ϵ_g and ϵ_h , and I is the identity matrix. If we assume that $f(x)$ has strict saddles (see Definition 1), a second-order stationary point is a local minimizer. In order to obtain a sub-optimal solution x which satisfies (3), some works explicitly calculate the eigenvector direction corresponding to the most negative eigenvalue of the Hessian matrix $\nabla^2 f(x)$ around saddle points, such as the cubic regularized Newton's (CRN) methods (Nesterov, 2006; Agarwal et al., 2017; Reddi et al., 2018; Tripuraneni et al., 2018; Zhou et al., 2018b; Curtis et al., 2017). The CRN-based methods require an *oracle* to compute the search direction at each iteration, where the oracle is difficult to derive and time-consuming to compute. Thus, some other works including this present work develop perturbation-based methods to escape saddle points.

Some perturbation-based methods rely on the strategy of injecting isotropic noise along the search direction, such as in the perturbed GD (PGD) and perturbed SGD (PSGD) methods (Ge et al., 2015; Jin et al., 2017; Zhang et al., 2017). A recent work observes that the stochasticity in SGD steps induces intrinsic anisotropic noise around saddle points, and hence proposes to utilize this noise by running a separate SGD step to escape saddle points (Daneshmand et al., 2018). The advantage of such a method is that the anisotropic noise does not reduce along the negative curvature around saddle points when the deep neural network (the size of the optimization problem) becomes massive. Thus, this leads to two new methods both based on the assumption called the correlated negative curvature (CNC), namely, the CNC-GD and CNC-SGD methods.

Although the anisotropy of the noise in SGD steps has been extensively studied (Zhu et al., 2019; Daneshmand et al., 2018; Simsekli et al., 2019), there are discrepancies in the discussion. Fang et al. (2019) assumes dispersive noise structure in SGD, such as the structure of Gaussian noise or uniform ball-shaped noise, which then supports the explicit uniform ball-shaped noise injection procedure in the PGD method (Jin et al., 2017). Although this assumption of dispersive (similar to isotropic) noise enables the authors to analyze SGD directly, it deserves a second thought. The variance of Gaussian noise or

uniform ball-shaped noise diminishes to zero along the negative curvature when the problem size increases, but practically the noise induced by SGD steps does not. For example, Daneshmand et al. (2018) experimentally show that the variance of noise caused by SGD along the negative curvature direction is not influenced by the dimension of deep neural networks. More importantly, Simsekli et al. (2019) have studied the long tail behavior of noise from SGD in deep neural networks and shown that the noise in SGD does not follow the behavior of Gaussian noise as well as uniform ball-shaped noise. Hence, we assume in this paper that SGD satisfies the CNC condition which has been theoretically proved for the non-convex half-space learning problems.

Algorithm 1 Finding a second-order stationary point

Require: ϵ_g and ϵ_h

- 1: **for** $k = 0, 1, 2, \dots$ **do**
- 2: $y^k = \text{Gradient-Focused-Optimizer}(x^{k-1})$
- 3: $x^k = \text{Escaping-Saddle-Algorithm}(y^k)$
- 4: **if** (ϵ_g, ϵ_h) -second-order conditions **then**
- 5: Return x^k
- 6: **end if**
- 7: **end for**

For perturbation-based algorithms, we summarize them into a general framework as in Algorithm 1. The procedure *Gradient-Focused-Optimizer*(\cdot) in Line 2 can be any algorithm that converges to an ϵ -first-order stationary point, such as, the GD, SGD, and stochastically controlled stochastic gradient (SCSG) methods. The procedure *Escaping-Saddle-Algorithm*(\cdot) in Line 3 is for escaping from the region around saddle points (also called the stuck region), typically by taking a negative curvature direction explicitly or implicitly. A few prior works attempted to use variance reduction methods in the *Gradient-Focused-Optimizer*(\cdot) (Xu et al., 2018; Allen-Zhu and Li, 2018; Zhou et al., 2018a) to reach a better convergence rate for second-order stationary points, but they have not been used in the *Escaping-Saddle-Algorithm*(\cdot). We are the first work to use variance reduced methods inside *Escaping-Saddle-Algorithm*(\cdot).

Our contributions. In this paper, we first propose a variance reduced algorithm, which we call CNC-SCSG, to escape strict saddle points by incorporating SGD into SCSG. We show that it converges to a second-order stationary point with a convergence rate faster than that of the CNC-SGD and comparable to that of the CNC-GD, under the assumption of the CNC condition. The computational complexity in terms of the number of IFO calls (see Definition 3) has also been analyzed. Comparing with GD methods, perturbed by either Gaussian noise or one SGD step, our simulation studies show that the CNC-SCSG converges in much fewer epochs than the perturbed GD methods even though they theoretically have comparable convergence rate. Furthermore, we generalize the CNC-SCSG into a framework that separates the part for escaping saddle points from the main algorithm so that it can be combined with any existing first-order algorithm, providing a mechanism that allows further search for faster convergence.

2. Related works

We briefly review the existing methods for finding second-order stationary points in the following three lines.

Perturbation methods. A line of research finds second-order stationary points by injecting perturbation when the algorithm gets close to saddle points. The perturbation can be either an explicit isotropic noise injected to the current gradient or search direction (Ge et al., 2015; Jin et al., 2017, 2018; Xu et al., 2018; Allen-Zhu and Li, 2018; Allen-Zhu, 2017; Jin et al., 2019; Fang et al., 2019), or a SGD step introducing intrinsic and anisotropic noise implicitly (Daneshmand et al., 2018).

As in the PSGD (Ge et al., 2015; Jin et al., 2019; Fang et al., 2019), PGD (Jin et al., 2017) and perturbed AGD (PAGD) (Jin et al., 2018) methods, researchers have shown that the stuck region is a “thin pancake”. Thus injecting random noise to gradients can help the algorithm to jump out of the stuck region with high probability. However, because the noise is isotropic, this strategy is inefficient in high dimension. The Neon (Xu et al., 2018) and Neon2 (Allen-Zhu and Li, 2018) methods connected the noise perturbed methods PGD and PSGD to the search methods of negative curvature direction, such as the power method (Kuczyński and Woźniakowski, 1992) and Oja’s method (Oja, 1982). These methods for the first time successfully separated the *Escaping-Saddle-Algorithm*(\cdot) from the main GD process. Because of the separation, the frameworks are easy to incorporate any suitable algorithm for *Gradient-Focused-Optimizer*(\cdot). The overall convergence rate has less dependence on the dimension d , i.e. from $poly(d)$ in PSGD (Ge et al., 2015) to $poly(\log(d))$ (Xu et al., 2018; Allen-Zhu and Li, 2018). Nevertheless, as the convergence rate still depends on d , it may cause issues in deep learning models with massive network parameters. Recently, (Daneshmand et al., 2018) observed that SGD works very well in deep learning applications, and experimentally showed that the anisotropic noise created by SGD has a high variance along the negative curvature direction. The variance does not diminish with the increase in the size of deep neural networks. This observation implies that SGD satisfies the CNC condition (see Definition 2). Hence, a single step of SGD can be used to escape saddle points, which can also remove the dependency on problem dimension as well.

Cubic regularized Newton’s (CRN) methods. Another line of studies for escaping saddle points is based on the CRN method (Nesterov, 2006) and its variants (Agarwal et al., 2017; Reddi et al., 2018; Tripuraneni et al., 2018; Zhou et al., 2018b; Curtis et al., 2017). These methods use second-order information directly. The CRN method (Nesterov, 2006) can converge to an $(\epsilon, \sqrt{\epsilon})$ -second-order stationary point in $O(\epsilon^{-\frac{3}{2}})$ steps, if there is an oracle which can return an update direction h at each iteration to minimize the cubic function $m(h) = g^T h + \frac{1}{2} h^T H h + \frac{\rho}{6} \|h\|^3$, where $g = \nabla f(x)$, $H = \nabla^2 f(x)$ and ρ is the second-order smoothness parameter of f . The FastCubic method in (Agarwal et al., 2017) improved the CRN method and achieved a better convergence rate. Its stochastic version has also been proposed by computing stochastic gradient and Hessian using two mini-batches respectively at each iteration (Tripuraneni et al., 2018). The SVRCubic method (Zhou et al., 2018b) introduced the variance reduction technique to the stochastic CRN method to reach the convergence rate of its deterministic version.

Stochastic variance reduction methods. For convex optimization, variance reduction methods have been extensively studied, such as, the stochastic variance reduced gradient (SVRG) (Johnson and Zhang, 2013), stochastically controlled stochastic gradient (SCSG) (Lei and Jordan, 2017), and stochastic average gradient (SAGA) (Defazio et al., 2014) methods, and they are well-known for faster convergence rates. In non-convex optimization, variance reduction methods have been proved to converge to ϵ -first-order stationary points (Reddi et al., 2016; Lei et al., 2017). Some of these methods have been used in the *Gradient-Focused-Optimizer*(\cdot) step of Algorithm 1 to find second-order stationary points (Xu et al., 2018; Allen-Zhu and Li, 2018; Zhou et al., 2018a).

3. Preliminaries

We use uppercase letters, e.g. A , to denote matrices and lowercase letters, e.g. x , to denote vectors. We use $\|\cdot\|$ to denote the 2-norm for vectors and the spectral norm for matrices, and $\lambda_{\min}(\cdot)$ to denote the minimum eigenvalue. For two matrices A and B , $A \succeq B$ iff $A - B$ is positive semi-definite. In this paper, the notation $O(\cdot)$ is used to hide constants which do not rely on the setup of the problem parameters and the notation $\tilde{O}(\cdot)$ is used to hide all ϵ -independent constants. The operator $E[\cdot]$ represents taking the expectation over all randomness, $[n]$ denotes the integer set $\{1, \dots, n\}$, $\nabla f(\cdot)$, $\nabla f_I(\cdot)$ and $\nabla f_z(\cdot)$ are the full gradient, the stochastic gradient over a mini-batch $I \subset [n]$ and the stochastic gradient over a single training example indexed by $z \in [n]$, respectively. We also assume that the probability of observing z given the model parameter x , $P(z|x) \propto \exp^{-f_z(x)}$.

Definition 1 (*Strict saddle*) *A twice differential function f has strict saddle if all its local minima have $\nabla^2 f(x) \succ 0$ and all its other stationary points satisfy that $\lambda_{\min}(\nabla^2 f(x)) < 0$.*

Definition 2 (*CNC-condition*) *A differentiable finite-sum function $f(x) : \mathbb{R}^d \rightarrow \mathbb{R}$ satisfies the CNC condition if $\exists \tau \geq 0$, s.t. $E[\langle \mathbf{v}_x, \nabla f_z(x) \rangle^2] \geq \tau$, $\forall x \in \{x : \lambda_{\min}(\nabla^2 f(x)) < 0\}$ and $z \in [n]$, where \mathbf{v}_x is the eigenvector corresponding to the minimum eigenvalue $\lambda_{\min}(\nabla^2 f(x))$ and $E[\cdot]$ is the expectation taken over the random sample z .*

Definition 3 (*Incremental First-order Oracle (IFO)*(Agarwal and Bottou, 2015)) *An IFO is a subroutine that takes a point $x \in \mathbb{R}^d$ and an index $z \in [n]$ and returns a pair $(f_z(x), \nabla f_z(x))$.*

Definition 4 (*Geometric distribution*) *A random variable N is said to follow a geometric distribution $\text{Geom}(\gamma)$ for some $\gamma > 0$, denoted as $N \sim \text{Geom}(\gamma)$, if N is a non-negative integer and the probability $P(N = k) = (1 - \gamma)\gamma^k$ for all $k = 0, 1, \dots$. It holds that $E[N] = \frac{\gamma}{1-\gamma}$.*

In this paper, we assume that the function $f(x)$ is lower-bounded by a constant f^* , which is the optimal value of the objective. As commonly used in the related works on escaping saddle points, we also assume that the gradient and Hessian of f_z are locally stable (Assumption 1 (1)-(2)), and the variance of the stochastic gradients is bounded from above (Assumption 1 (3)).

Assumption 1 *The twice differentiable function $f_z(x)$, $z \in [n]$, satisfies:*

1. L -Lipschitz gradient, i.e., $\|\nabla f_z(x_1) - \nabla f_z(x_2)\| \leq L\|x_1 - x_2\|, \forall x_1, x_2 \in \mathbb{R}^d$;
2. ρ -Lipschitz Hessian, i.e., $\|\nabla^2 f_z(x_1) - \nabla^2 f_z(x_2)\| \leq \rho\|x_1 - x_2\|, \forall x_1, x_2 \in \mathbb{R}^d$;
3. $\exists l \geq 0$, such that, $\|\nabla f_z(x)\| \leq l, \forall x \in \mathbb{R}^d$, and $\forall z \in [n]$.

We further exploit the observation given in (Daneshmand et al., 2018) that SGD steps intrinsically induce anisotropic noise and the variance of noise along negative curvature direction does not decrease with the increase of deep neural network dimension size. We emphasize that the original CNC-condition in (Daneshmand et al., 2018) does not necessarily hold for the entire x domain. It only needs to hold at the points around strict saddle points for SGD to jump out of stuck regions.

Assumption 2 *In Problem (1), we assume that $f(x)$ satisfies the CNC-condition at points in the stuck regions.*

The CNC-condition can be regarded as instability of the iteration dynamics in SGD around strict saddle points. Unlike the methods of injecting isotropic noise to the first order algorithms as in Ge et al. (2015); Jin et al. (2017, 2018); Xu et al. (2018); Allen-Zhu and Li (2018) which have a convergence rate dependent on the dimension d (i.e., either $poly(d)$ or $poly \log(d)$), the most important advantage of using the anisotropic noise induced by SGD is that the convergence rate no longer depends on the dimension d . When optimizing deep neural networks with millions of parameters, the anisotropic noise provided by SGD can have a significant advantage over injected isotropic noise.

Remark 5 *Around saddle points, the variance-covariance matrix of the stochastic gradient $\nabla f_z(x)$ is approximately equal to the empirical Fisher’s information matrix (see Appendix E). In practice, under the assumptions that the sample size n is large enough and the current x is not too far away from the ground truth parameter, Fisher’s information matrix $E_{P(z|x)}[\nabla^2 \log(P(z|x))]$ approximately equals to the Hessian matrix H of $f(\cdot)$ at x (Note that taking logarithm of the likelihood $\prod_{z=1}^n P(z|x)$ yields a finite sum f). Thus, the intrinsic noise in SGD is naturally embedded into the Hessian information of f (Zhu et al., 2019). This explains the anisotropic behavior of the noise in SGD.*

4. The CNC-SCSG algorithm

In this section, we present a novel algorithm CNC-SCSG (Algorithm 2), which utilizes SCSG and SGD to escape strict saddle points and is able to find $(\epsilon, \sqrt{\rho}\epsilon^{\frac{2}{5}})$ -second-order stationary points. The SCSG algorithm is a member of the SVRG family, which was first proposed in Lei and Jordan (2017) and showed competitive time complexity in convex optimization. Later it was extended to non-convex optimization (Lei et al., 2017). The original SVRG method computes a full gradient before starting an inner loop which typically contains $O(n)$ iterations. The SCSG differs from the SVRG mainly because the number of iterations in the inner loop is stochastically determined by an integer sampled from $Geom(\gamma)$ where γ is related to the size b of the mini-batch I used in the inner loop.

Algorithm 2 CNC-SCSG

Require: \mathcal{K}_{thres} , stepsizes η, r , accuracy ϵ and epoch T

```

1:  $t_{noise} = 0$ 
2: for  $k = 0, 1, 2, \dots, T$  do
3:    $\tilde{\mu} = 1/n \sum_{i=1}^n \nabla f_i(\tilde{x}^k)$ 
4:   if  $t_{noise} \geq \mathcal{K}_{thres}$  &&  $\|\tilde{\mu}\| \leq \epsilon$  then
5:     Randomly pick  $i \in \{1, \dots, n\}$ 
6:      $\tilde{x}^k = \tilde{x}^k - r(\nabla f_i(\tilde{x}^k))$ 
7:      $t_{noise} = 0$ 
8:      $\tilde{\mu} = 1/n \sum_{i=1}^n \nabla f_i(\tilde{x}^k)$ 
9:   end if
10:   $x_0^k = \tilde{x}^k$ 
11:  Generate  $N_k \sim \text{Geom}(n/(n+b))$ 
12:  for  $t = 1, 2, \dots, N_k$  do
13:    Sample  $I_t \subset \{1, \dots, n\}$ , where  $|I_t| = b$ 
14:     $x_t^k = x_{t-1}^k - \eta(\nabla f_{I_t}(x_{t-1}^k) - \nabla f_{I_t}(\tilde{x}^k) + \tilde{\mu})$ 
15:  end for
16:  set  $\tilde{x}^{k+1} = x_t^k$ 
17:   $t_{noise} = t_{noise} + 1$ 
18: end for
    
```

As shown in Algorithm 2, our algorithm consists of an outer loop (Lines 2-18) and an inner loop (Lines 12-15). In each iteration of the outer loop, a full gradient is calculated (Line 3). Following SCSG, an integer is sampled from a geometric distribution and then used as the number of iterations in the inner loop (Line 11). Variance reduction steps (Lines 13 - 14) are commonly used in the family of SVRG. More importantly, Lines 4-9 are the steps for escaping saddle points where Line 4 is used to determine if the ϵ -first-order stationary condition ($\|\tilde{\mu}\| \leq \epsilon$) is satisfied; if yes, and the escaping-saddle-point steps have not been invoked in the past \mathcal{K}_{thres} epochs, perturbation by one step of SGD (Line 6) is taken. t_{noise} is a counter counting the number of epochs after a perturbation and the threshold parameter \mathcal{K}_{thres} is algorithm-specific (to be discussed in proofs). Theoretically, a parameter f_{thres} specifying the desirable decrease of function value should be provided to terminate the algorithm. In other words, we run \mathcal{K}_{thres} epochs after the SGD perturbation step, and then check if the objective f decreases less than f_{thres} ; if yes, terminate and the algorithm arrives at an $(\epsilon, \sqrt{\rho}\epsilon^{\frac{2}{5}})$ -second-order stationary point. In practice, there is no need to specify the value of f_{thres} , and we can terminate the algorithm when f does not decrease for a couple of epochs.

Convergence analysis. We first prove in Theorem 6 that the CNC-SCSG (Algorithm 2) converges to a second-order stationary point of Problem (1) within a finite number of epochs with high probability. We then derive the convergence rate and computational complexity in Theorem 7.

Theorem 6 *Under Assumptions 1 and 2, Algorithm 2 obtains an $(\epsilon, \sqrt{\rho}\epsilon^{\frac{2}{5}})$ -second-order stationary point within $T = \frac{b}{n} \frac{288CC_1l^4(f(x_0)-f^*)}{C_2\delta\eta^2\tau^2\epsilon^2} \log(\frac{1}{\sqrt{\rho}\epsilon^{\frac{2}{5}}})$ epochs with probability at least*

$1 - \delta$, where $\eta L = \gamma(\frac{b}{n})^{\frac{2}{3}}$, $b \leq \frac{n}{8}$, $C = b[\frac{(b - \frac{\eta^2 L^2 n - \eta n)(1 - \eta L)}{1 + 2\eta} - \frac{L^3 \eta^2 n}{2b}]^{-1}$, γ and C_1 are constants independent of ϵ , and $C_2 = \min(\frac{1}{2}, \frac{\eta}{C_L})$.

The proof of Theorem 6 is sketched in Section 6 and its complete proof is provided in Appendix B.

Theorem 7 *Under the same assumptions of Theorem 6, the convergence rate is $\tilde{O}(\epsilon^{-2} \log(1/\epsilon))$. If we further require $b = \frac{n}{C_4}$, where $C_4 \geq 8$ is a constant and is independent of n , the expectation of overall computational complexity (i.e., the number of IFO calls) is $O(n\epsilon^{-2} \log(1/\epsilon))$.*

Provided that the constants C , C_1 , C_2 and γ in Theorem 6 are independent of ϵ , the number of iterations to reach convergence is $E[\sum_{k=1}^T N_k] = \frac{n}{b} T = \tilde{O}(\epsilon^{-2} \log(1/\epsilon))$. If we further require $C_4 = \frac{n}{b}$ to be a constant independent of n , the number of epochs T only depends on $\frac{1}{C_4} = \frac{b}{n}$. Therefore, the number of IFO calls can be derived by $E[\sum_{k=1}^T (n + bN_k)] = 2nT = O(n\epsilon^{-2} \log(1/\epsilon))$.

5. A general framework for CNC-SCSG

In this section, we reorganize the CNC-SCSG algorithm (Algorithm 2) into a general framework - Algorithm 4, similar to Neon (Xu et al., 2018) or Neon2 (Allen-Zhu and Li, 2018), which allows to employ any first order stochastic algorithm \mathcal{A} to speed up the process of finding second-order stationary points. We interpret algorithm \mathcal{A} as an ‘‘epoch’’ based algorithm. For example, algorithm \mathcal{A} can be one epoch of SVRG, n steps of SGD or one

Algorithm 3 CNC-SCSG-Escaping

Require: x , \mathcal{K}_{thres} , stepsize η and r

- 1: Randomly pick $i \in \{1, \dots, n\}$ and update weight
- 2: $\tilde{x}^0 = x - r(\nabla f_i(x))$
- 3: **for** $k = 0, 1, 2, \dots, \mathcal{K}_{thres}$ **do**
- 4: $\tilde{\mu} = 1/n \sum_{i=1}^n \nabla f_i(\tilde{x}^k)$
- 5: $x_0^k = \tilde{x}^k$
- 6: Generate $N_k \sim \text{Geom}(n/(n+b))$
- 7: **for** $t = 1, 2, \dots, N_k$ **do**
- 8: Randomly pick $I_t \subset \{1, \dots, n\}$
- 9: $x_t^k = x_{t-1}^k - \eta(\nabla f_{I_t}(x_{t-1}^k) - \nabla f_{I_t}(\tilde{x}^k) + \tilde{\mu})$
- 10: **end for**
- 11: set $\tilde{x}^{k+1} = x_t^k$
- 12: **end for**
- 13: $y = \tilde{x}^{\mathcal{K}_{thres}+1}$

step of GD. If we run \mathcal{A} of SGD for instance, we do not mean the entire SGD process, but n steps of SGD, and hence reasonably assume that the number of IFO calls $T_{\mathcal{A}}$ for algorithm \mathcal{A} is upper bounded by $O(n)$. Note that Algorithm 2 consists of two parts: 1) the SGD perturbation step (Lines 4-9) to inject noise and the \mathcal{K}_{thres} SCSG epochs following this

perturbation step; 2) the remaining SCSG epochs. The first part can be taken out to form Algorithm 3, and will be triggered whenever an ϵ_g -first-order stationary point is satisfied in the main Algorithm 4. The whole algorithm terminates when the first-order condition is satisfied and f decreases less than f_{thres} .

In Algorithm 4, the first-order algorithm \mathcal{A} is applied to decrease the function value in each epoch k , until the norm of the gradient becomes small. Once a critical point y_k s.t. $\|\nabla f(y_k)\| \leq \epsilon_g$ is reached, Algorithm 3 is invoked, and returns a new iterate x_k , which guarantees a sufficient decrease in the value of f , unless y_k is already an (ϵ_g, ϵ_h) -second-order stationary point. This general framework, similar to Neon and Neon2, also requires the evaluation of the first-order condition (Line 4). For stochastic algorithms that do not compute full gradients, a few approximation schemes have been developed to effectively check the first-order condition (Xu et al., 2018; Allen-Zhu and Li, 2018) (see Appendix C).

Algorithm 4 \mathcal{A} with CNC-SCSG

Require: ϵ_g, ϵ_h , stepsize η and r

- 1: $\mathcal{K}_{thres} \leftarrow \tilde{O}(\epsilon_h^{-1} \log(\epsilon_h^{-1}))$ $f_{thres} \leftarrow \tilde{O}(\epsilon_h^4)$
- 2: **for** $k = 0, 1, 2, \dots$ **do**
- 3: $y_k = \mathcal{A}(x_k)$
- 4: **if** ϵ_g -first-order condition **then**
- 5: $x_k = \text{CNC-SCSG-Escaping}(y_k, \mathcal{K}_{thres}, \eta, r)$
- 6: **if** $f(y_k) - f(x_k) \leq f_{thres}$ **then**
- 7: return y_k
- 8: **end if**
- 9: **else**
- 10: $x_k = y_k$
- 11: **end if**
- 12: **end for**

Remark 8 *The framework facilitates searching for a better dimension-free convergence rate, and enjoys the same benefit as in Neon (Xu et al., 2018) and Neon2 (Allen-Zhu and Li, 2018). But they contain parameters, e.g., t and \mathcal{F} in the Neon, and T and a distance r in the Neon2, which so far there is no knowledge on how to set up in practice. For the CNC-SCSG, only \mathcal{K}_{thres} is required to set up and f_{thres} can be omitted in practice. We will provide a guidance in Section 6.*

Convergence analysis. We first guarantee that there is a sufficient decrease in the function value whenever the CNC-SCSG-Escaping procedure (Algorithm 3) is invoked.

Lemma 9 *Under Assumptions 1 and 2, and $\lambda_{\min}(\nabla^2 f(x)) \leq \epsilon_h$, in $\mathcal{K}_{thres} = \hat{O}(\epsilon_h^{-1} \log(\epsilon_h^{-1}))$ epochs, Algorithm 3 returns y , where $f(x) - f(y) \geq \frac{\eta r^2 \epsilon_h^4}{144l^4 \rho^2 C} \min(\frac{1}{2}, \frac{\eta}{CL})$. The expected decrease of function value per epoch is lower bounded by $D_e = \tilde{O}(\epsilon_h^5 \log^{-1}(\epsilon_h^{-1}))$.*

Lemma 9 guarantees in expectation that the decrease of function value per epoch around strict saddle points is at least D_e . Then if we assume that i) when $\|\nabla f(x)\| > \epsilon_g$, in expectation \mathcal{A} drops function value by $D_{\mathcal{A}(\epsilon_g)}$ per epoch, and ii) when $\|\nabla f(x)\| \leq \epsilon_g$ and

$\lambda_{\min}(\nabla^2 f(x)) \leq \epsilon_h$, \mathcal{A} is stable, i.e., does not increase function value too much in expectation, we can obtain the following convergence result by setting $g_{thres} = \min(D_e, D_{\mathcal{A}(\epsilon_g)})$. Its proof is similar to that of Theorem 6 and has been moved to Appendix.

Theorem 10 *Given Assumptions 1 and 2, a first order algorithm \mathcal{A} and $y = \mathcal{A}(x)$ such that:*

$$\begin{aligned} \|\nabla f(x)\| \geq \epsilon_g &\Rightarrow E[f(y) - f(x)] \leq -D_{\mathcal{A}(\epsilon_g)}, \\ \|\nabla f(x)\| \leq \epsilon_g &\Rightarrow E[f(y) - f(x)] \leq \frac{\min(D_e, D_{\mathcal{A}(\epsilon_g)})\delta}{2}, \end{aligned}$$

Algorithm 4 converges to an (ϵ_g, ϵ_h) -second-order stationary point in $T = \tilde{O}(\max(\frac{1}{D_e}, \frac{1}{D_{\mathcal{A}(\epsilon_g)}}))$ epochs with probability $1 - \delta$.

Theorem 11 *Assume all the assumptions in Theorem 10 hold, the computational complexity (i.e., the number of IFO calls) is $O(\max(\frac{1}{D_e}, \frac{1}{D_{\mathcal{A}(\epsilon_g)}}) \cdot (\max(T_e, +T_{check}/\mathcal{K}_{thres}, T_{\mathcal{A}} + T_{check})))$, where T_e is the number of IFO calls of Algorithm 3 per epoch, $T_{\mathcal{A}}$ is the number of IFO calls of \mathcal{A} per epoch, and T_{check} is the number of IFO calls of checking the first-order stationary condition.*

The computational cost T_{check} of checking first-order stationary condition can be considered either in one epoch of \mathcal{A} or in \mathcal{K}_{thres} epochs of SCSG in Algorithm 3. Therefore, the upper bound on the number of IFO calls per epoch, including those of Line 4 in Algorithm 4, is $\max(T_e + T_{check}/\mathcal{K}_{thres}, T_{\mathcal{A}} + T_{check})$. The computational complexity follows from multiplying the above bound with the number of epochs in Theorem 10. Note that there exist many first-order algorithms satisfying the requirements of algorithm \mathcal{A} . For completeness, we provide an exemplar algorithm in Appendix D.

6. Proof sketches

Table 1: Constraints for parameters used in the proof

Notation	Constraint Requirements	Reference
ϵ_g	$\epsilon_g = \epsilon$	
ϵ_h	$\epsilon_h = (\rho\epsilon)^{\frac{2}{5}}$	
γ	$\gamma \leq \min\{\eta_0 L(\frac{n}{b})^{\frac{2}{3}}, \frac{1}{3}\}$	
η	$\eta = L\gamma^{\frac{b}{3}}$	SCSG stepsize
r	$r \leq \min(\frac{1}{2}, \frac{\eta}{CL}) \frac{\tau}{12\rho l^3} \epsilon_h^2$	SGD stepsize
f_{thres}	$f_{thres} \leq \frac{\eta r r \epsilon_h^2}{12l\rho C}$	Lemma 13
\mathcal{K}_{thres}	$\mathcal{K}_{thres} \geq \frac{C_1}{\eta \epsilon_h} \frac{b}{n} \log(\frac{1}{\epsilon_h})$	Lemma 13
g_{thres}	$g_{thres} \leq \frac{\gamma}{5L} (\frac{n}{b})^{\frac{1}{3}} \epsilon_g^2$	Inequality (4)
g_{thres}	$g_{thres} \geq \frac{10l^2\gamma^2}{L\delta} (\frac{b}{n})^{\frac{1}{3}}$	Inequality (6)
g_{thres}	$g_{thres} \leq \frac{n}{b} \frac{\eta^2 \epsilon_h^3 \tau r}{C_1 12l\rho C} \log^{-1}(\frac{1}{\epsilon_h})$	Inequality (5)

In order to prove Theorem 6, we consider three types of epochs based on the magnitude of the gradient and the most negative eigenvalue of Hessian matrix at each snapshot \tilde{x}^k for $k = 1, 2, 3, \dots$: i) \tilde{x}^k with large gradient $\|\nabla f(\tilde{x}^k)\| \geq \epsilon_g$; ii) \tilde{x}^k with large negative curvature $\lambda_{\min}(\nabla^2 f(\tilde{x}^k)) \leq -\epsilon_h$; and iii) \tilde{x}^k satisfying neither of them. The following analysis is epoch-based and mainly inspired by the paper (Daneshmand et al., 2018), but our analysis based on SCSG is more difficult. The theoretical analysis is based on a specific setup for hyper-parameters, as summarized in Table 1. Proofs of the lemmas used in this section have been moved to Appendix.

Regime with large gradients. Considering that ϵ_g -first-order condition is not satisfied at \tilde{x}^k , we can get the expected function value decrease per epoch at large gradient regime as in the following lemma:

Lemma 12 *With conditions: $\eta L = \gamma(\frac{b}{n})^{\frac{2}{3}}$ where $b \geq 1$, $n \geq 8b$ and $\gamma \leq \frac{1}{3}$ and assumption that ϵ_g -first-order condition is not satisfied, the decrease of function value per epoch satisfies that $E[f(\tilde{x}^k) - f(\tilde{x}^{k-1})] \leq -\frac{\gamma}{5L}(\frac{n}{b})^{\frac{1}{3}}\epsilon_g^2$.*

By setting parameter $g_{thres} \leq \frac{\gamma}{5L}(\frac{n}{b})^{\frac{1}{3}}\epsilon_g^2$, we further have that

$$E[f(\tilde{x}^k) - f(\tilde{x}^{k-1})] \leq -g_{thres}, \quad (4)$$

which implies the average decrease of function value for each epoch is no smaller than g_{thres} .

Regime with large negative curvatures. In this part, we establish the number of epochs (\mathcal{K}_{thres}) required for a significant decrease of function value (f_{thres}) around strict saddle points.

Lemma 13 *If the Hessian matrix at \tilde{x}^0 has a small negative eigenvalue, i.e. $\lambda_{\min}(\nabla^2 f(\tilde{x}^0)) \leq -\epsilon_h$, $f_{thres} \leq \frac{\eta\tau r\epsilon_h^2}{12l\rho C}$ and $\mathcal{K}_{thres} \geq \frac{C_1}{\eta\epsilon_h} \frac{n}{b} \log(\frac{1}{\epsilon_h})$, where C_1 is a sufficient large constant and independent of ϵ_h , the expectation of the function value decrease is $E[f(\tilde{x}^0) - f(\tilde{x}^{\mathcal{K}_{thres}})] \geq f_{thres}$.*

After imposing constraints that $f_{thres} \leq \frac{\eta\tau r\epsilon_h^2}{12l\rho C}$ and $\mathcal{K}_{thres} \geq \frac{C_1}{\eta\epsilon_h} \frac{n}{b} \log(\frac{1}{\epsilon_h})$, we can find constraint for average decrease of function value per epoch:

$$g_{thres} = \frac{f_{thres}}{\mathcal{K}_{thres}} \leq \frac{n}{b} \frac{\eta^2\epsilon_h^3\tau r}{12l\rho C C_1} \log^{-1}\left(\frac{1}{\epsilon_h}\right). \quad (5)$$

Regime satisfying neither of above. We prove that the function value around a second-order stationary point does not increase too much due to disturbance.

Lemma 14 *Given that $\eta L = \gamma(\frac{b}{n})^{\frac{2}{3}}$, where $b \geq 1$, $n \geq 8b$ and $\gamma \leq \frac{1}{3}$, for each epoch of the SCSG, the increase of function value caused by disturbance is, $E[f(\tilde{x}^k) - f(\tilde{x}^{k-1})] \leq \frac{5l^2\gamma^2}{L}(\frac{b}{n})^{\frac{1}{3}}$.*

By setting parameter $g_{thres} \geq \frac{10l^2\gamma^2}{L\delta}(\frac{b}{n})^{\frac{1}{3}}$, we can further obtain that:

$$E[f(\tilde{x}^k) - f(\tilde{x}^{k-1})] \leq \frac{\delta g_{thres}}{2}. \quad (6)$$

Proof sketch of Theorem 6 With appropriate values of γ and C_1 , we have that $g_{thres} = \frac{n}{b} \frac{\eta^2 \epsilon_b^3 \tau r}{C_1 12 l \rho C} \log^{-1}(\frac{1}{\epsilon_h})$ and Inequalities (4), (5) and (6) hold. We define event $A_t := \{\|\nabla f(\tilde{x}^t)\| \geq \epsilon_g \text{ or } \lambda_{min}(\nabla^2 f(\tilde{x}^t)) \leq -\epsilon_h\}$. Let R be a random variable representing the ratio of second-order stationary points visited by our algorithm at snapshots in the past T epochs. That is, $R = \frac{1}{T} \sum_{t=1}^T \mathbf{I}(A_t^c)$, where $\mathbf{I}(\cdot)$ is an indicator function. Let P_t be the probability that A_t occurs and $1 - P_t$ be the probability that its complement A_t^c occurs. Our goal is that $E(R) = \frac{1}{T} \sum_{t=1}^T (1 - P_t)$ holds with high probability. That is, $E(R) = \frac{1}{T} \sum_{t=1}^T (1 - P_t) \geq 1 - \delta$, or $\frac{1}{T} \sum_{t=1}^T P_t \leq \delta$.

Unfortunately, estimating the probabilities P_t for $t \in \{1, \dots, T\}$ is very difficult. However, we successfully obtain an upper bound: $\frac{1}{T} \sum_{t=1}^T P_t \leq \frac{f(x_0) - f^*}{T g_{thres}} + \frac{\delta}{2}$. Then by letting $\frac{f(x_0) - f^*}{T g_{thres}} + \frac{\delta}{2} \leq \delta$, we have that

$$T = \frac{2(f(x_0) - f^*)}{\delta g_{thres}} = \frac{b}{n} \frac{288 C C_1 l^4 (f(x_0) - f^*)}{C_2 \delta \eta^2 \tau^2 \epsilon^2} \log\left(\frac{1}{\sqrt{\rho} \epsilon^{\frac{2}{5}}}\right).$$

7. Empirical evaluations

In this section, we present simulation results to verify that the proposed CNC-SCSG can escape saddle points faster than its competitors. In the simulations, we consider the following nonconvex finite-sum problem: $\min_{x \in \mathbb{R}^d} f(x) = \frac{1}{n} \sum_{i=1}^n \frac{1}{1 + \exp(-y_i z_i^T x)} + \lambda \sum_{j=1}^d \frac{x_j^2}{1 + x_j^2}$ where $y_i \in \{0, 1\}$ denotes the label, $z_i \in \mathbb{R}^d$ denotes the feature data of the i^{th} data point and λ is a positive trade-off parameter. Data points $\{z_i\}$ with labels $y_i=0$ were generated from a normal distribution $N(\mu_0=\mathbf{0}, I)$ while data points $\{z_i\}$ with labels $y_i=1$ were generated from $N(\mu_1=\mathbf{1}, I)$. The efficiency for escaping saddle points is measured by the number of epochs each algorithm uses for the escape.

We generated two simulation datasets: a low dimensional dataset with $n = 40$ and $d = 4$, and a high dimensional dataset with $n = 200$ and $d = 20$. We compared CNC-SCSG with three algorithms PGD (Jin et al., 2017), CNC-SGD and CNC-GD (Daneshmand et al., 2018). We did not include Neon-based (Neon2-based) algorithms (Xu et al., 2018; Allen-Zhu and Li, 2018) because Neon (Neon2) so far provided no knowledge on how to set up the parameters t and F (T and a distance r , resp.) in practice, and no empirical tests of the full algorithms were given in their original papers except in Neon (simulation was given only around saddle points which did not involve t and F). However, without t and F (T and r), we cannot correctly implement the algorithm for comparison. The complete experimental setups for each of the tested algorithms can be found in Appendix A.

Results. As shown in Figure 1, for the tested datasets, our proposed CNC-SCSG algorithm consistently used significantly smaller epochs to escape saddle points comparing with PGD and CNC-GD. For example in Figure 1(a), for the saddle point at objective value around 2.2, CNC-GD and PGD used ~ 250 and ~ 350 epochs to escape it respectively while CNC-SCSG used only ~ 10 epochs. Compared with CNC-SGD, CNC-SCSG have comparable numbers of epochs although in theory its convergence rate is better than CNC-SGD. We conjecture that it is because the objective function tested in the simulation is relatively simple and has a small number of intervals with large gradients. As in Figure 1(c) and (d), we also observed that CNC-based algorithms including CNC-SCSG are more

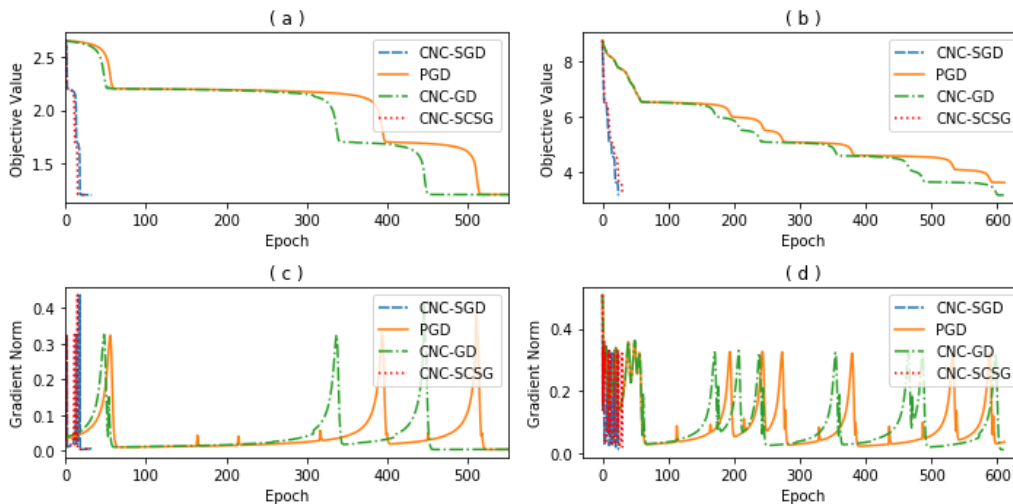


Figure 1: Comparison of different methods on a synthetic problem. Plots (a) and (b) correspond to the objective value over the increase of epochs and plots (c) and (d) correspond to the gradient norm over number of epochs. Plots (a) and (c) are for the low dimension dataset, and plots (b) and (d) are for the high dimension dataset.

stable than isotropic noise perturbed algorithm PGD, by noticing that PGD shows spikes in both simulations.

Remark 15 *Considering that N_k can be large, wasting stochastic gradient calculation may occur. Though Algorithm 2 theoretically requires the first-order condition check (in the proof), in practice we can remove the checking and insert one step SGD for every t_{thres} iteration, where t_{thres} is moderately smaller than n , e.g. $n/4$. Hence, Lines 4-9 and Line 17 in Algorithm 2 can be moved into inner loop when first condition requirement check is removed. without hurting the algorithm due to the stability of SGD. (unlike PGD shows spikes in Figure 1 (c) and (d))*

8. Conclusion

We propose the CNC-SCSG algorithm to escape saddle points for nonconvex optimization so it converges to second-order stationary points. The CNC-SCSG algorithm can achieve the same convergence rate as CNC-GD. We also generalize the CNC-SCSG algorithm into a framework like the Neon or Neon2 method, which can be readily used in conjunction with any existing algorithm that converges to first-order stationary points. We observe that in all existing first-order oracle algorithms, when to break from the escaping process and the evaluation of conditions for second-order stationary points can be issues due to heavy dependence on algorithm parameters, which are often clueless to find appropriate values in practical non-convex optimization problems. We will investigate this problem as the future work.

Acknowledgments

This work was funded by NSF grants CCF-1514357, DBI-1356655, and IIS-1718738 to Jinbo Bi, who was also supported by NIH grants K02-DA043063 and R01-DA037349.

References

- Alekh Agarwal and Leon Bottou. A lower bound for the optimization of finite sums. In *International Conference on Machine Learning*, pages 78–86, 2015.
- Naman Agarwal, Zeyuan Allen-Zhu, Brian Bullins, Elad Hazan, and Tengyu Ma. Finding approximate local minima faster than gradient descent. In *Proceedings of the 49th Annual ACM SIGACT Symposium on Theory of Computing*, pages 1195–1199. ACM, 2017.
- Zeyuan Allen-Zhu. Natasha: Faster non-convex stochastic optimization via strongly non-convex parameter. In *Proceedings of the 34th International Conference on Machine Learning-Volume 70*, pages 89–97. JMLR. org, 2017.
- Zeyuan Allen-Zhu. Natasha 2: Faster non-convex optimization than sgd. In *Advances in Neural Information Processing Systems*, pages 2676–2687, 2018.
- Zeyuan Allen-Zhu and Yuanzhi Li. Neon2: Finding local minima via first-order oracles. In *Advances in Neural Information Processing Systems*, pages 3720–3730, 2018.
- Animashree Anandkumar and Rong Ge. Efficient approaches for escaping higher order saddle points in non-convex optimization. In *Conference on Learning Theory*, pages 81–102, 2016.
- Yair Carmon, John C Duchi, Oliver Hinder, and Aaron Sidford. Convex until proven guilty: Dimension-free acceleration of gradient descent on non-convex functions. In *Proceedings of the 34th International Conference on Machine Learning-Volume 70*, pages 654–663. JMLR. org, 2017.
- Yair Carmon, John C Duchi, Oliver Hinder, and Aaron Sidford. Accelerated methods for nonconvex optimization. *SIAM Journal on Optimization*, 28(2):1751–1772, 2018.
- Frank E Curtis, Daniel P Robinson, and Mohammadreza Samadi. A trust region algorithm with a worst-case iteration complexity of $o(\epsilon^{-3/2})$ for nonconvex optimization. *Mathematical Programming*, 162(1-2):1–32, 2017.
- Hadi Daneshmand, Jonas Kohler, Aurelien Lucchi, and Thomas Hofmann. Escaping saddles with stochastic gradients. In *International Conference on Machine Learning*, pages 1163–1172, 2018.
- Aaron Defazio, Francis Bach, and Simon Lacoste-Julien. Saga: A fast incremental gradient method with support for non-strongly convex composite objectives. In *Advances in neural information processing systems*, pages 1646–1654, 2014.

- Cong Fang, Chris Junchi Li, Zhouchen Lin, and Tong Zhang. Spider: Near-optimal non-convex optimization via stochastic path-integrated differential estimator. In *Advances in Neural Information Processing Systems*, pages 686–696, 2018.
- Cong Fang, Zhouchen Lin, and Tong Zhang. Sharp analysis for nonconvex sgd escaping from saddle points. *arXiv preprint arXiv:1902.00247*, 2019.
- Rong Ge, Furong Huang, Chi Jin, and Yang Yuan. Escaping from saddle points online stochastic gradient for tensor decomposition. In *Conference on Learning Theory*, pages 797–842, 2015.
- Lan Guanghui Ghadimi, Saeed. Accelerated gradient methods for nonconvex nonlinear and stochastic programming. *Mathematical Programming*, 156(1-2):59–99, 2016.
- Saeed Ghadimi, Guanghui Lan, and Hongchao Zhang. Mini-batch stochastic approximation methods for nonconvex stochastic composite optimization. *Mathematical Programming*, 155(1-2):267–305, 2016.
- Chi Jin, Rong Ge, Praneeth Netrapalli, Sham M Kakade, and Michael I Jordan. How to escape saddle points efficiently. In *Proceedings of the 34th International Conference on Machine Learning-Volume 70*, pages 1724–1732. JMLR. org, 2017.
- Chi Jin, Praneeth Netrapalli, and Michael I Jordan. Accelerated gradient descent escapes saddle points faster than gradient descent. In *Conference On Learning Theory*, pages 1042–1085, 2018.
- Chi Jin, Praneeth Netrapalli, Rong Ge, Sham M Kakade, and Michael I Jordan. Stochastic gradient descent escapes saddle points efficiently. *arXiv preprint arXiv:1902.04811*, 2019.
- Rie Johnson and Tong Zhang. Accelerating stochastic gradient descent using predictive variance reduction. In *Advances in neural information processing systems*, pages 315–323, 2013.
- Jacek Kuczynski and Henryk Woźniakowski. Estimating the largest eigenvalue by the power and lanczos algorithms with a random start. *SIAM journal on matrix analysis and applications*, 13(4):1094–1122, 1992.
- Lihua Lei and Michael Jordan. Less than a single pass: Stochastically controlled stochastic gradient. In *Artificial Intelligence and Statistics*, pages 148–156, 2017.
- Lihua Lei, Cheng Ju, Jianbo Chen, and Michael I Jordan. Non-convex finite-sum optimization via scsg methods. In *Advances in Neural Information Processing Systems*, pages 2348–2358, 2017.
- Polyak Boris T Nesterov, Yurii. Cubic regularization of newton method and its global performance. *Mathematical Programming*, 108(1):177–205, 2006.
- Yurii Nesterov. *Introductory lectures on convex optimization: A basic course*, volume 87. Springer Science & Business Media, 2013.

- Erkki Oja. Simplified neuron model as a principal component analyzer. *Journal of mathematical biology*, 15(3):267–273, 1982.
- Sashank Reddi, Manzil Zaheer, Suvrit Sra, Barnabas Poczos, Francis Bach, Ruslan Salakhutdinov, and Alex Smola. A generic approach for escaping saddle points. In *International Conference on Artificial Intelligence and Statistics*, pages 1233–1242, 2018.
- Sashank J Reddi, Ahmed Hefny, Suvrit Sra, Barnabas Poczos, and Alex Smola. Stochastic variance reduction for nonconvex optimization. In *International conference on machine learning*, pages 314–323, 2016.
- Umut Simsekli, Levent Sagun, and Mert Gurbuzbalaban. A tail-index analysis of stochastic gradient noise in deep neural networks. In *International Conference on Machine Learning*, pages 5827–5837, 2019.
- Nilesh Tripuraneni, Mitchell Stern, Chi Jin, Jeffrey Regier, and Michael I Jordan. Stochastic cubic regularization for fast nonconvex optimization. In *Advances in Neural Information Processing Systems*, pages 2904–2913, 2018.
- Yi Xu, Jing Rong, and Tianbao Yang. First-order stochastic algorithms for escaping from saddle points in almost linear time. In *Advances in Neural Information Processing Systems*, pages 5535–5545, 2018.
- Yuchen Zhang, Percy Liang, and Moses Charikar. A hitting time analysis of stochastic gradient langevin dynamics. *Proceedings of Machine Learning Research* vol, 65:1–43, 2017.
- Dongruo Zhou, Pan Xu, and Quanquan Gu. Finding local minima via stochastic nested variance reduction. *arXiv preprint arXiv:1806.08782*, 2018a.
- Dongruo Zhou, Pan Xu, and Quanquan Gu. Stochastic variance-reduced cubic regularized newton method. In *International Conference on Machine Learning*, pages 5985–5994, 2018b.
- Zhanxing Zhu, Jingfeng Wu, Bing Yu, Lei Wu, and Jinwen Ma. The anisotropic noise in stochastic gradient descent: Its behavior of escaping from sharp minima and regularization effects. In *International Conference on Machine Learning*, pages 7654–7663, 2019.

Appendix A. Comparison of algorithms for non-convex optimization

Table 2: Algorithms for Non-convex Optimization

Guarantees	Oracle	Algorithm	ϵ_g	ϵ_h	Time Complexity (iteration \cdot Oracle/iter)	Dependence
First-order Stationary Point	Gradient	GD; SGD (Nesterov, 2013)	ϵ	no	$O(\epsilon^{-2}) \cdot O(n)$; $O(\epsilon^{-4}) \cdot O(1)$	N/A
		AGD; SAGD (Ghadimi, 2016)	ϵ	no	$O(\epsilon^{-2}) \cdot O(n)$; $O(\epsilon^{-4}) \cdot O(1)$	N/A
		Guarded-AGD (Carmon et al., 2017)	ϵ	no	$O(\epsilon^{-\frac{7}{4}} \log(\epsilon^{-1})) \cdot O(n)$	N/A
		SVRG (Reddi et al., 2016)	ϵ	no	$O(\epsilon^{-2}) \cdot O(n)$	N/A
		SCSG (Lei et al., 2017)	ϵ	no	$O(\min(\epsilon^{-\frac{10}{3}}, n^{\frac{2}{3}} \epsilon^{-2}))$	N/A
2nd-order Stationary Point (Local Minimum)	Gradient	PSGD (Ge et al., 2015)	ϵ	$\sqrt{\rho\epsilon}$	$O(\epsilon_g^{-4}) \cdot O(1)$	$poly(d)$
		PGD (Jin et al., 2017)	ϵ	$\sqrt{\rho\epsilon}$	$O(\epsilon^{-2} \log(\frac{d}{\epsilon})) \cdot O(n)$	$poly \log(d)$
		PAGD (Jin et al., 2018)	ϵ	$\sqrt{\rho\epsilon}$	$O(\epsilon^{-\frac{7}{4}} \log^6(\frac{d}{\epsilon})) \cdot O(n)$	$poly \log(d)$
		CNC-PGD (Daneshmand et al., 2018)	ϵ	$\sqrt{\rho\epsilon}^{\frac{2}{5}}$	$O(\epsilon^{-2} \log(\epsilon^{-1})) \cdot O(n)$	free
		CNC-PSGD (Daneshmand et al., 2018)	ϵ	$\sqrt{\rho\epsilon}^{\frac{2}{5}}$	$O(\epsilon^{-4} \log^2(\epsilon^{-1})) \cdot O(1)$	free
		NEON+SVRG (Xu et al., 2018)	ϵ	$\epsilon^{\frac{1}{2}}$	$O(n^{\frac{2}{3}} \epsilon^{-2} + n \epsilon^{-\frac{3}{2}} + \epsilon^{-\frac{11}{3}})$	$poly \log(d)$
		NEON2+CDHS (Allen-Zhu and Li, 2018)	ϵ_g	ϵ_h	$O(n^{\frac{2}{3}} \epsilon_g^{-2} + n \epsilon_h^{-3} + n^{\frac{3}{4}} \epsilon_h^{-\frac{7}{2}})$	$poly \log(d)$
		Natasha2 by (Allen-Zhu, 2018)	ϵ_g	ϵ_h	$O(\epsilon_h^{-5} + \epsilon^{-\frac{13}{4}} + \epsilon_g^{-3} \epsilon_h^{-1})$	$poly \log(d)$
		SPIDER+NEON2 (Fang et al., 2018)	ϵ	$\epsilon^{\frac{1}{2}}$	$O(\min(n^{\frac{1}{2}} \epsilon^{-2} + \epsilon^{-\frac{5}{2}}, \epsilon^{-3}))$	$poly \log(d)$
	SNVRG+NEON2 (Zhou et al., 2018a)	ϵ_g	ϵ_h	$O(n^{\frac{1}{2}} \epsilon_g^{-2} + n \epsilon_h^{-3} + n^{\frac{3}{4}} \epsilon_h^{-\frac{7}{2}})$	$poly \log(d)$	
	Hessian-vector	NCD+AGD(Carmon et al., 2018)	ϵ	$\epsilon^{\frac{1}{2}}$	$O(\epsilon^{-\frac{7}{4}} \log(\epsilon^{-1})) \cdot T_{Hv}$	N/A
		FastCubic by (Agarwal et al., 2017)	ϵ	$\epsilon^{\frac{1}{2}}$	$O(\epsilon^{-\frac{3}{2}} n + \epsilon^{-\frac{7}{4}} n^{\frac{3}{4}}) \cdot T_{Hv}$	N/A
		SCubic by (Tripuraneni et al., 2018)	ϵ	$\sqrt{\rho\epsilon}$	$O(\epsilon^{-\frac{7}{2}}) \cdot T_{Hv}$	N/A
		SVRCubic by (Zhou et al., 2018b)	ϵ	$\sqrt{\rho\epsilon}$	$O(\epsilon^{-\frac{3}{2}}) \cdot T_{cubic}$	N/A
	Hessian	Cubic Alg (Nesterov, 2006)	ϵ	$\sqrt{\epsilon}$	$O(\epsilon^{-\frac{3}{2}}) \cdot T_{cubic}$	N/A
Trust Region (Curtis et al., 2017)		ϵ	$\sqrt{\epsilon}$	$O(\epsilon^{-\frac{3}{2}}) \cdot T_H$	N/A	

Here T_{Hv} is the time for a Hessian vector product oracle and it is $O(d)$ as discussed by (Agarwal et al., 2017), and T_{cubic} is the time for each iteration of the cubic algorithm. Under the strict saddle point assumption, any second-order stationary point will be a local minimizer. Additionally, $\|\nabla f(x)\| \leq \epsilon_g$, $\lambda_{min}(\nabla^2 f(x)) \geq -\epsilon_h$, and N/A means not defined in the corresponding reference.

Appendix B. The experimental setup

In order to demonstrate the efficiency of anisotropic noise generated by SGD for high dimensional data, we generated two simulation datasets: I) a low dimensional dataset with $n = 40$ and $d = 4$; and II) a high dimensional dataset with $n = 200$ and $d = 20$. For both datasets, $\lambda = 0.5$. The stepsizes for both SCSG and GD are 0.5, and the stepsizes for the SGD in both CNC-SCSG and CNC-GD are 2. Noise for PGD was uniformly drawn from the sphere of an Euclidean ball with radius 0.05. When the first order condition is satisfied, noise injection or a SGD jumping step was taken only if they had not been taken in the previous 50 iterations.

Appendix C. Detailed proofs

C.1 Proofs of lemmas

Lemma 16 *For all $0 < \beta < 1$, we have bounded series:*

$$\sum_{i=1}^t (1 + \beta)^{t-i} \leq 2\beta^{-1}(1 + \beta)^t; \quad (7)$$

$$\sum_{i=1}^t i(1 + \beta)^{t-i} \leq 2\beta^{-2}(1 + \beta)^t. \quad (8)$$

Proof From Taylor expansion, for any $|z| < 1$, we have:

$$\begin{aligned} \sum_{k=1}^{\infty} (z)^k &\leq 1/(1 - z); \\ \sum_{k=1}^{\infty} k(z)^k &\leq z/(1 - z)^2. \end{aligned}$$

■

Lemma 17 *Let $x_j \in \mathbb{R}^d$ be an arbitrary population of M vectors with*

$$\sum_{j=1}^M x_j = 0.$$

Further let J be a uniform random subset of $\{1, 2, \dots, M\}$ with size m . Then

$$E\left[\left\|\frac{1}{m} \sum_{j \in J} x_j\right\|^2\right] = \frac{M - m}{(M - 1)m} \frac{1}{M} \sum_{j=1}^M \|x_j\|^2 \leq \frac{\mathbf{I}(m < M)}{m} \frac{1}{M} \sum_{j=1}^M \|x_j\|^2,$$

where $\mathbf{I}(\cdot)$ is an indicator function.

Lemma 18 *Let $N \sim \text{Geom}(\gamma)$. Then for any sequences $\{D_i\}$,*

$$E[D_N - D_{N+1}] = \left(\frac{1}{\gamma} - 1\right)(D_0 - E[D_N]).$$

Both Lemmas 17 and 18 can reference (Lei et al., 2017) for proof.

C.2 One-epoch analysis for SCSG

The analysis for this section is inspired by (Lei et al., 2017) and is included here for completeness.

Lemma 19 Denote $v_t^k = \nabla f_{I_t}(x_t^k) - \nabla f_{I_t}(\tilde{x}) + \tilde{\mu}$ to be the updating direction at t -th iteration of k -th epoch, then

$$E_{I_t}[\|v_t^k\|^2] \leq \frac{L^2}{b} \|x_t^k - x_0^k\|^2 + \|\nabla f(x_t^k)\|^2. \quad (9)$$

Proof Let $\xi_t^k = \nabla f_{I_t}(x_t^k) - \nabla f(x_t^k) - (\nabla f_{I_t}(\tilde{x}) - \tilde{\mu})$, easily derive $E_{I_t}[\xi_t^k] = 0$.

$$\begin{aligned} E_{I_t}[\|v_t^k\|^2] &= E_{I_t}[\|\nabla f_{I_t}(x_t^k) - \nabla f_{I_t}(x_0^k) - (\nabla f(x_t^k) - \nabla f(x_0^k)) + \nabla f(x_t^k)\|^2] \\ &= E_{I_t}[\|\xi_t^k + \nabla f(x_t^k)\|^2] \\ &= E_{I_t}[\|\xi_t^k\|^2] + 2 \langle E_{I_t}[\xi_t^k], \nabla f(x_t^k) \rangle + \|\nabla f(x_t^k)\|^2 \\ &= E_{I_t}[\|\xi_t^k\|^2] + \|\nabla f(x_t^k)\|^2 \end{aligned}$$

By Lemma 17:

$$\begin{aligned} E_{I_t}[\|\xi_t^k\|^2] &= E_{I_t}[\|\nabla f_{I_t}(x_t^k) - \nabla f_{I_t}(x_0^k) - (\nabla f(x_t^k) - \nabla f(x_0^k))\|^2] \\ &\leq \frac{1}{b} \frac{1}{n} \sum_{i=1}^n \|\nabla f_{z_i}(x_t^k) - \nabla f_{z_i}(x_0^k) - (\nabla f(x_t^k) - \nabla f(x_0^k))\|^2 \\ &= \frac{1}{bn} \left(\sum_{z=1}^n \|\nabla f_z(x_t^k) - \nabla f_z(x_0^k)\|^2 - \|(\nabla f(x_t^k) - \nabla f(x_0^k))\|^2 \right) \\ &\leq \frac{1}{bn} \sum_{z=1}^n \|\nabla f_z(x_t^k) - \nabla f_z(x_0^k)\|^2 \\ &\leq \frac{L^2}{b} \|x_t^k - x_0^k\|^2, \end{aligned}$$

where the first inequality is due to Lemma 17 and last inequality is due to L-smoothness. \blacksquare

Lemma 20 Suppose $\eta L < 1$, then we can get

$$\eta n(1 - \eta L) E[\|\nabla f(\tilde{x}^k)\|^2] \leq bE[f(\tilde{x}^{k-1}) - f(\tilde{x}^k)] + \frac{L^3 \eta^2 n}{2b} E[\|\tilde{x}^k - \tilde{x}^{k-1}\|^2]. \quad (10)$$

Proof

$$\begin{aligned} E_{I_t}[f(x_{t+1}^k)] &\leq f(x_t^k) - \eta \|\nabla f(x_t^k)\|^2 + \frac{L\eta^2}{2} E_{I_t}[\|v_t^k\|^2] \\ &\leq f(x_t^k) - \eta \left(1 - \frac{\eta L}{2}\right) \|\nabla f(x_t^k)\|^2 + \frac{L^3 \eta^2}{2b} \|x_t^k - x_0^k\|^2 \\ &\leq f(x_t^k) - \eta(1 - \eta L) \|\nabla f(x_t^k)\|^2 + \frac{L^3 \eta^2}{2b} \|x_t^k - x_0^k\|^2, \end{aligned}$$

where the first inequality is due to L-smoothness and the second inequality is due to Lemma 19.

Let E_k denotes the expectation over all mini-batches I_0, I_1, \dots of epoch k given N_k . Hence,

$$\eta(1 - \eta L)E_k[\|\nabla f(x_t^k)\|^2] \leq E_k[f(x_t^k)] - E_k[f(x_{t+1}^k)] + \frac{L^3\eta^2}{2b}E_k[\|x_t^k - x_0^k\|^2].$$

Let $t = N_k$. By taking expectation with respect to N_k and using Fubini's theorem, we obtain that

$$\begin{aligned} \eta(1 - \eta L)E_{N_k}E_k[\|\nabla f(x_{N_k}^k)\|^2] &\leq E_{N_k}(E_k[f(x_{N_k}^k)] - E_k[f(x_{N_k+1}^k)]) + \frac{L^3\eta^2}{2b}E_{N_k}E_k[\|x_{N_k}^k - x_0^k\|^2] \\ &= \frac{b}{n}(f(x_0^k) - E_kE_{N_k}[f(x_{N_k}^k)]) + \frac{L^3\eta^2}{2b}E_kE_{N_k}[\|x_{N_k}^k - x_0^k\|^2], \end{aligned}$$

where the equality is due to Lemma 18.

Replace $x_{N_k}^k, x_0^k$ with $\tilde{x}_{k+1}, \tilde{x}_k$, we get the desired inequality. \blacksquare

Lemma 21 *Suppose $\eta^2 L^2 < \frac{b^2}{n}$, then*

$$(b - \frac{\eta^2 L^2 n}{b})E[\|\tilde{x}^k - \tilde{x}^{k-1}\|^2] \leq -2\eta n E[\langle \nabla f(\tilde{x}^k), \tilde{x}^k - \tilde{x}^{k-1} \rangle] + 2\eta^2 n E[\|\nabla f(\tilde{x}^k)\|^2]. \quad (11)$$

Proof

$$\begin{aligned} &E_{I_t}[\|x_{t+1}^k - x_0^k\|^2]E_{I_t}[\|x_t^k - \eta v_t^k - x_0^k\|^2] \\ &= \|x_t^k - x_0^k\|^2 - 2\eta \langle E_{I_t}[v_t^k], x_t^k - x_0^k \rangle + \eta^2 E_{I_t}[\|v_t^k\|^2] \\ &= \|x_t^k - x_0^k\|^2 - 2\eta \langle \nabla f(x_t^k), x_t^k - x_0^k \rangle + \eta^2 E_{I_t}[\|v_t^k\|^2] \\ &\leq (1 + \frac{\eta^2 L^2}{b})\|x_t^k - x_0^k\|^2 - 2\eta \langle \nabla f(x_t^k), x_t^k - x_0^k \rangle + \eta^2 \|\nabla f(x_t^k)\|^2 \\ &\leq (1 + \frac{\eta^2 L^2}{b})\|x_t^k - x_0^k\|^2 - 2\eta \langle \nabla f(x_t^k), x_t^k - x_0^k \rangle + 2\eta^2 \|\nabla f(x_t^k)\|^2. \end{aligned}$$

where first inequality dues to Lemma 19 and second inequality is for future convenience.

Using the same notation E_k as in previous lemma, we get:

$$2\eta E_k[\langle \nabla f(x_t^k), x_t^k - x_0^k \rangle] \leq (1 + \frac{\eta^2 L^2}{b})E_k[\|x_t^k - x_0^k\|^2] - E_k[\|x_{t+1}^k - x_0^k\|^2] + 2\eta^2 E_k[\|\nabla f(x_t^k)\|^2].$$

Then Let $t = N_k$. By taking expectation with respect to N_k and using Fubini's Theorem, we get

$$\begin{aligned} &2\eta E_{N_k}E_k[\langle \nabla f(x_{N_k}^k), x_{N_k}^k - x_0^k \rangle] \\ &\leq (1 + \frac{\eta^2 L^2}{b})E_{N_k}E_k[\|x_{N_k}^k - x_0^k\|^2] - E_{N_k}E_k[\|x_{N_k+1}^k - x_0^k\|^2] + 2\eta^2 E_{N_k}[\|\nabla f(x_{N_k}^k)\|^2] \\ &= (-\frac{b}{n} + \frac{\eta^2 L^2}{b})E_{N_k}E_k[\|x_{N_k}^k - x_0^k\|^2] + 2\eta^2 E_{N_k}[\|\nabla f(x_{N_k}^k)\|^2]. \end{aligned}$$

Replace $x_{N_k}^k, x_0^k$ with $\tilde{x}^{k+1}, \tilde{x}^k$, we get the desired result. \blacksquare

C.3 Lemmas for epochs with large gradient

Lemma 22 *With conditions: $\eta L = \gamma(\frac{b}{n})^{\frac{2}{3}}$ where $b \geq 1$, $n \geq 8b$ and $\gamma \leq \frac{1}{3}$, (Lei et al., 2017) guarantee the decrease of function value for each epoch:*

$$E[f(\tilde{x}^k) - f(\tilde{x}^{k-1})] \leq -\frac{\gamma}{5L} \left(\frac{n}{b}\right)^{\frac{1}{3}} E[\|\nabla f(\tilde{x}^k)\|^2].$$

Proof Lemma 20 Inequality (10) $\times 2$ + Lemma 21 Inequality (11) $\times \frac{b}{n\eta}$:

$$\begin{aligned} & 2\eta n \left(1 - \eta L - \frac{b}{n}\right) E[\|\nabla f(\tilde{x}^k)\|^2] + \frac{b^3 - \eta^2 L^2 b n - \eta^3 L^3 n^2}{b\eta n} E[\|\tilde{x}^k - \tilde{x}_{k-1}\|^2] \\ & \leq -2bE[\langle \nabla f(\tilde{x}^k), \tilde{x}^k - \tilde{x}_{k-1} \rangle] + 2bE[f(\tilde{x}^{k-1}) - f(\tilde{x}^k)] \\ & \leq \frac{b\eta n}{b^3 - \eta^2 L^2 b n - \eta^3 L^3 n^2} b^2 E[\|\nabla f(\tilde{x}^k)\|^2] + \frac{b^3 - \eta^2 L^2 b n - \eta^3 L^3 n^2}{b\eta n} E[\|\tilde{x}^k - \tilde{x}_{k-1}\|^2] \\ & \quad + 2bE[f(\tilde{x}^{k-1}) - f(\tilde{x}^k)]. \end{aligned}$$

Therefore:

$$\frac{\eta n}{b} \left(2 - \frac{2b}{n} - 2\eta L - \frac{b^3}{b^3 - \eta^2 L^2 b n - \eta^3 L^3 n^2}\right) E[\|\nabla f(\tilde{x}^k)\|^2] \leq 2E[f(\tilde{x}^{k-1}) - f(\tilde{x}^k)].$$

Since $\eta L = \gamma(\frac{b}{n})^{\frac{2}{3}}$ and $n \geq 8b \geq 8$:

$$b^3 - \eta^2 L^2 b n - \eta^3 L^3 n^2 \geq b^3 \left(1 - \frac{\gamma^2}{2} - \gamma^3\right).$$

Then we get:

$$\gamma \left(\frac{n}{b}\right)^{\frac{1}{3}} \left(2 - \frac{2b}{n} - 2\gamma \left(\frac{b}{n}\right)^{\frac{2}{3}} - \frac{1}{1 - \frac{\gamma^2}{2} - \gamma^3}\right) E[\|\nabla f(\tilde{x}^k)\|^2] \leq 2LE[f(\tilde{x}^{k-1}) - f(\tilde{x}^k)].$$

Considering $n \geq 8b \geq 8$ and $\gamma \leq \frac{1}{3}$, we get the final result. \blacksquare

C.4 Lemmas for epochs with small gradient but not around saddle points

Lemma 23 *With conditions: $\eta L = \gamma(\frac{b}{n})^{\frac{2}{3}}$ where $b \geq 1$, $n \geq 8b$ and $\gamma \leq \frac{1}{3}$, for each iteration of SCSG, the increase of function value caused by disturbance is:*

$$E[f(x_t) - f(x_{t-1})] \leq \frac{5l^2\gamma^2}{L} \left(\frac{b}{n}\right)^{\frac{4}{3}}.$$

Proof

$$\begin{aligned} E[\|\xi_t\|^2] &= E[\|\xi_t^k\|^2] \\ &= E[\|\nabla f(x_{t-1}^k) - \nabla f_{I_t}(x_{t-1}^k) + \nabla f_{I_t}(\tilde{x}^k) - \tilde{\mu}\|^2] \\ &\leq 2E[\|\nabla f(x_{t-1}^k) - \nabla f_{I_t}(x_{t-1}^k)\|^2 + \|\nabla f_{I_t}(\tilde{x}^k) - \tilde{\mu}\|^2] \\ &\leq 2E[\|\nabla f_{I_t}(x_{t-1}^k)\|^2 + \|\nabla f_{I_t}(\tilde{x}^k)\|^2] \\ &\leq 4l^2, \end{aligned}$$

where last inequality is due to the norm of gradient is l -bounded.

$$\begin{aligned}
 E[f(x_t) - f(x_{t-1})] &\leq -\eta \|\nabla f(x_{t-1})\|^2 + \frac{L}{2} \eta^2 E[\|\nabla f(x_{t-1}) + \xi_{t-1}\|^2] \\
 &\leq \frac{L}{2} \eta^2 E[\|\nabla f(x_{t-1}) + \xi_{t-1}\|^2] \\
 &\leq L\eta^2 E[\|\nabla f(x_{t-1})\|^2] + L\eta^2 E[\|\xi_{t-1}\|^2] \\
 &\leq 5Ll^2\eta^2 \\
 &= \frac{5l^2\gamma^2}{L} \left(\frac{b}{n}\right)^{\frac{4}{3}}.
 \end{aligned}$$

■

Lemma 24 *With conditions: $\eta L = \gamma \left(\frac{b}{n}\right)^{\frac{2}{3}}$ where $b \geq 1$, $n \geq 8b$ and $\gamma \leq \frac{1}{3}$, for each epoch of SCSG, the increase of function value caused by disturbance is:*

$$E[f(\tilde{x}^k) - f(\tilde{x}^{k-1})] \leq \frac{5l^2\gamma^2}{L} \left(\frac{b}{n}\right)^{\frac{1}{3}}.$$

Proof

$$\begin{aligned}
 E[f(\tilde{x}^k) - f(\tilde{x}^{k-1})] &= \sum_{t=1}^{N_k} E[f(x_t^{k-1}) - f(x_{t-1}^{k-1})] \\
 &\leq \frac{5l^2\gamma^2}{L} \left(\frac{b}{n}\right)^{\frac{4}{3}} E[N_k] \\
 &= \frac{5l^2\gamma^2}{L} \left(\frac{b}{n}\right)^{\frac{1}{3}}
 \end{aligned}$$

■

C.5 Lemmas for epochs around saddle points

The following representations are used to show different status of parameters in the following proof:

- x_t^k : parameter x at t -th iteration of k -th epoch;
- \tilde{x}^k : parameter x used to calculate full gradient at epoch k ;
- x_t : parameter x at t -th iteration, where t is the global counter;

Lemma 25 *Suppose $b \geq 1$, $n \geq 8b \geq 8$, then there exists a small stepsize η , such that*

$$E[\|\tilde{x}^k - \tilde{x}^{k-1}\|^2] \leq CE[f(\tilde{x}^{k-1}) - f(\tilde{x}^k)],$$

where $C = b \left[\frac{(b - \frac{\eta^2 L^2 n}{b} - \eta n)(1 - \eta L)}{1 + 2\eta} - \frac{L^3 \eta^2 n}{2b} \right]^{-1} > 0$.

Proof With Inequality (11) in Lemma 21 and $-2\langle a, b \rangle \leq \|a\|^2 + \|b\|^2$, we have:

$$\begin{aligned} \left(b - \frac{\eta^2 L^2 n}{b}\right) E[\|\tilde{x}^k - \tilde{x}^{k-1}\|^2] &\leq -2\eta n E[\langle \nabla f(\tilde{x}^k), \tilde{x}^k - \tilde{x}^{k-1} \rangle] + 2\eta^2 n E[\|\nabla f(\tilde{x}^k)\|^2] \\ &\leq \eta n E[\|\tilde{x}^k - \tilde{x}^{k-1}\|^2] + (\eta n + 2\eta^2 n) E[\|\nabla f(\tilde{x}^k)\|^2] \end{aligned}$$

Reorganize:

$$\left(b - \frac{\eta^2 L^2 n}{b} - \eta n\right) E[\|\tilde{x}^k - \tilde{x}^{k-1}\|^2] \leq (\eta n + 2\eta^2 n) E[\|\nabla f(\tilde{x}^k)\|^2].$$

With Inequality (10) in Lemma 20, we plug in the bound of $E[\|\nabla f(\tilde{x}^k)\|^2]$ and reorganize:

$$\frac{\left(b - \frac{\eta^2 L^2 n}{b} - \eta n\right)(\eta n(1 - \eta L))}{\eta n + 2\eta^2 n} E[\|\tilde{x}^k - \tilde{x}^{k-1}\|^2] \leq b E[f(\tilde{x}^{k-1}) - f(\tilde{x}^k)] + \frac{L^3 \eta^2 n}{2b} E[\|\tilde{x}^k - \tilde{x}^{k-1}\|^2].$$

Hence

$$E[\|\tilde{x}^k - \tilde{x}^{k-1}\|^2] \leq C E[f(\tilde{x}^{k-1}) - f(\tilde{x}^k)],$$

where $C = b \left[\frac{\left(b - \frac{\eta^2 L^2 n}{b} - \eta n\right)(1 - \eta L)}{1 + 2\eta} - \frac{L^3 \eta^2 n}{2b} \right]^{-1}$.

Then exist constant η_0 , for arbitrary $\eta \leq \eta_0$, the following inequality is true:

$$\frac{\left(b - \frac{\eta^2 L^2 n}{b} - \eta n\right)(1 - \eta L)}{1 + 2\eta} - \frac{L^3 \eta^2 n}{2b} > 0.$$

Therefore, there exist positive constant C , such that

$$E[\|\tilde{x}^k - \tilde{x}^{k-1}\|^2] \leq C E[f(\tilde{x}^{k-1}) - f(\tilde{x}^k)].$$

Let's argue the existence of η_0 :

$$\begin{aligned} h(\eta) &= \frac{\left(b - \frac{\eta^2 L^2 n}{b} - \eta n\right)(1 - \eta L)}{1 + 2\eta} - \frac{L^3 \eta^2 n}{2b} \\ &= \frac{b + \Theta(\eta) + O(\eta)}{1 + 2\eta}. \end{aligned}$$

Hence,

$$\lim_{\eta \rightarrow +0} h(\eta) = b.$$

Given that $h(\eta)$ is continuous in $(0, 1]$, there must exist η_0 , such that for arbitrary $\eta \leq \eta_0$,

$$f(\eta) > 0. \quad \blacksquare$$

We want to see significant decrease in function values f_{thres} in every \mathcal{K}_{thres} epochs, not only when in the scenario where gradients is large, but also when the smallest eigenvalue of hessian matrix is strictly small. The proof is finished by contradiction: first assume the

decrease of function value is lower-bounded, then derive an upper bound and a lower bound, then contradiction is introduced by let lower bound larger than upper bound. Hence, the decrease of function value is larger than f_{thres} .

Without loss generality, \tilde{x}^0 satisfies first-order stationary condition, which is the starting point of escaping saddle points stage and is followed by one step SGD and \mathcal{K}_{thres} epoch of SCSG.

Lemma 26 *Suppose that expectation of the decrease function value is lower-bounded:*

$$E[f(\tilde{x}^{\mathcal{K}})] - f(\tilde{x}^0) \geq -f_{thres}. \quad (12)$$

Then, the expectation of the distance from the current $\tilde{x}^{\mathcal{K}}$ to \tilde{x}^0 is bounded as

$$E[\|\tilde{x}^{\mathcal{K}} - \tilde{x}^0\|^2] \leq 2\mathcal{K}Cf_{thres} + \mathcal{K}CL(lr)^2 + 2(lr)^2. \quad (13)$$

Proof

$E[f(\tilde{x}^{\mathcal{K}}) - f(\tilde{x}^0)]$ can be split into two parts: the first step for SGD : $\tilde{x}^{(1)} = \tilde{x}^0 - r\nabla f(\tilde{x}^0)$ and the remaining $\mathcal{K} - 1$ epochs SCSG, $\tilde{x}^{(1)}, \dots, \tilde{x}^{(\mathcal{K})}$.

For inserting SGD step:

$$E[f(\tilde{x}^1) - f(\tilde{x}^0)] \leq -r\|\nabla f(\tilde{x}^0)\|^2 + \frac{L(lr)^2}{2} \leq \frac{L(lr)^2}{2}. \quad (14)$$

By Lemma 25, we can bound the expected distance in the parameter space for remaining $\mathcal{K} - 1$ epochs of SCSG:

$$\begin{aligned} E[\|\tilde{x}^{\mathcal{K}} - \tilde{x}^1\|^2] &\leq (\mathcal{K} - 1) \sum_{k=1}^{\mathcal{K}-1} E[\|\tilde{x}^{k+1} - \tilde{x}^k\|^2] \\ &\leq \mathcal{K} \sum_{k=1}^{\mathcal{K}-1} CE[(f(\tilde{x}^k) - f(\tilde{x}^{k+1}))] \\ &\leq \mathcal{K}CE[(f(\tilde{x}^1) - f(\tilde{x}^{\mathcal{K}}))] \\ &\leq \mathcal{K}CE[(f(\tilde{x}^0) - f(\tilde{x}^{\mathcal{K}}) + f(\tilde{x}^1) - f(\tilde{x}^0))] \\ &\leq \mathcal{K}Cf_{thres} + \frac{\mathcal{K}CL(lr)^2}{2} \end{aligned}$$

The last inequality is due to assumption 12 and inequality 14.

Replace the above inequality into the following bound:

$$\begin{aligned} E[\|\tilde{x}^{\mathcal{K}} - \tilde{x}^0\|^2] &= 2(E[\|\tilde{x}^{\mathcal{K}} - \tilde{x}^1\|^2] + E[\|\tilde{x}^1 - \tilde{x}^0\|^2]) \\ &\leq 2(\mathcal{K}Cf_{thres} + \frac{\mathcal{K}CL(lr)^2}{2} + (lr)^2) \\ &\leq 2\mathcal{K}Cf_{thres} + \mathcal{K}CL(lr)^2 + 2(lr)^2. \end{aligned}$$

Hence, we obtain upper bound for $E[\|\tilde{x}^{\mathcal{K}} - \tilde{x}^0\|^2]$. ■

Lemma 27 [Distance Upper Bound] Suppose that expectation of the decrease function value is lower-bounded:

$$E[f(\tilde{x}^{\mathcal{K}})] - f(\tilde{x}^0) \geq -f_{thres}.$$

Then, the expectation of the distance from the current iterate x_{t+1} to \tilde{x}^0 is bounded as

$$E[\|x_{t+1} - \tilde{x}^0\|^2] \leq 4\mathcal{K}Cf_{thres} + 2\mathcal{K}CL(lr)^2 + 4(lr)^2 + 2(l\eta)^2 \quad (15)$$

where t is a global iteration counter and $t = \sum_{k=1}^{\mathcal{K}-1} N_k$.

Proof From x_t (or $\tilde{x}^{(\mathcal{K})}$) to x_{t+1} is one step of full gradient.

$$\begin{aligned} E[\|x_{t+1} - \tilde{x}^0\|^2] &\leq 2E[\|x_{t+1} - x_t\|^2] + 2E[\|x_t - \tilde{x}^0\|^2] \\ &= 2E[\eta^2\|\nabla f(x_t)\|^2] + 2E[\|\tilde{x}^{\mathcal{K}} - \tilde{x}^0\|^2] \\ &\leq 2(l\eta)^2 + 4\mathcal{K}Cf_{thres} + 2\mathcal{K}CL(lr)^2 + 4(lr)^2 \end{aligned}$$

Hence, we obtain upper bound for $E[\|x_{t+1} - \tilde{x}^0\|^2]$. ■

In the following part, we also want to obtain upper bound for $E[\|x_{t+1} - \tilde{x}^0\|^2]$. The following part analysis is iteration based, where $t = \sum_{k=1}^{\mathcal{K}-1} N_k$. We use x_0 to denote \tilde{x}^0 without ambiguity.

Lemma 28 (Nesterov, 2013) [Taylor expansion bound for the gradient By Nesterov] For every twice differentiable function $f : \mathbb{R}^d \rightarrow \mathbb{R}$ with ρ -Lipshitz Hessians, the following bound holds true:

$$\|\nabla f(x) - \nabla f(x_0)\| \leq \frac{\rho}{2}\|x - x_0\|^2,$$

where

$$g(x) := f(x_0) + (x - x_0)^T \nabla f(x_0) + \frac{1}{2}(x - x_0)^T H(x - x_0),$$

where $H = \nabla^2 f(x_0)$ and x is close enough to x_0 .

Let's work on lower bound of $E[\|x_{t+1} - x_0\|^2]$.

$$\begin{aligned} x_{t+1} - x_0 &= x_t - x_0 - \eta \nabla f(x_t) + \eta \xi_t \\ &= x_t - x_0 - \eta \nabla g_t + \eta (\nabla g_t - \nabla f(x_t) + \xi_t) \\ &\downarrow \text{replace } \nabla g_t = \nabla f(x_0) + H(x - x_0) \\ &= (I - \eta H)(x_t - x_0) + \eta (\nabla g_t - \nabla f(x_t) - \nabla f(x_0) + \xi_t) \\ &= (I - \eta H)^t(x_1 - x_0) + \eta \left(\sum_{k=1}^t (I - \eta H)^{t-k} (\nabla g_k - \nabla f_k) \right. \\ &\quad \left. - \sum_{k=1}^t (I - \eta H)^{t-k} \nabla f(x_0) + \sum_{k=1}^t (I - \eta H)^{t-k} \xi_k \right) \\ &= u_t + \eta (\delta_t + d_t + \zeta_t), \end{aligned}$$

where

$$u_t := (I - \eta H)^t(x_1 - x_0);$$

$$\begin{aligned}\delta_t &:= \sum_{k=1}^t (I - \eta H)^{t-k} (\nabla g(x_k) - \nabla f(x_k)); \\ d_t &:= -\sum_{k=1}^t (I - \eta H)^{t-k} \nabla f(x_0); \\ \zeta_t &:= \sum_{k=1}^t (I - \eta H)^{t-k} \xi_k.\end{aligned}$$

Then,

$$\begin{aligned}E[\|x_{t+1} - x_0\|^2] &= E[\|u_t + \eta(\delta_t + d_t + \zeta_t)\|^2] \\ &\geq E[\|u_t\|^2] + 2\eta E[u_t^T \delta_t] + 2\eta E[u_t^T d_t] + 2\eta E[u_t^T \zeta_t] \\ &\geq E[\|u_t\|^2] - 2\eta E[\|u_t\|] E[\|\delta_t\|] + 2\eta E[u_t^T d_t] + 2\eta E[u_t^T] E[\zeta_t].\end{aligned}$$

Lemma 29 (*Removing initial gradient dependency*).

$$E[u_t]^T d_t \geq 0. \quad (16)$$

Proof

$$E[u_t] = (I - \eta H)^t E[x_1 - x_0] = -r(I - \eta H)^t \nabla f(x_0).$$

Since $I - \eta H \succeq 0$,

$$\begin{aligned}E[u_t]^T d_t &= r((I - \eta H)^t \nabla f(x_0))^T \sum_{k=1}^t (I - \eta H)^{t-k} \nabla f(x_0) \\ &= r \sum_{k=1}^t \nabla f(x_0)^T (I - \eta H)^{2t-k} \nabla f(x_0) \\ &\geq 0.\end{aligned}$$

■

Lemma 30 (*Exponential Growing Power Iteration*). *After the SCSG runs t steps, it yields an exponentially growing lower bound on the expected squared norm of u_t as follows:*

$$E[\|u_t\|^2] \geq \tau r^2 \kappa^{2t}. \quad (17)$$

Proof Let v represents the eigenvector corresponding to the most negative eigenvalue $\lambda_{\min}(H)$,

$$E[\|u_t\|^2] = E[\|v\|^2 \|u_t\|^2] \geq E[(v^T u_t)^2].$$

Suppose $H = U^T \Sigma U$, then $(I - \eta H) = U^T (I - \eta \Sigma) U$. Further, we have:

$$v^T (I - \eta H) = v^T (1 - \eta \lambda_{\min}(H)) = v^T (1 + \eta \lambda).$$

Finally, we get:

$$E[\|u_t\|^2] \geq r^2 (1 + \eta \lambda)^{2t} E[(v^T \nabla f_z(x_0))^2] \geq \tau r^2 (\kappa)^{2t}$$

where $\kappa = (1 + \eta \lambda)$ and $E[(v^T \nabla f_z(x_0))^2] \geq \tau$ is CNC-assumption. ■

Remark 31 We know $\lambda \geq \epsilon_h$, due to negative curvature assumption.

Lemma 32 The norm of u_t is deterministically bounded as

$$\|u_t\| \leq rl\kappa^t. \quad (18)$$

Proof

$$\begin{aligned} \|u_t\| &= \|(I - \eta H)^t(x_1 - x_0)\| \\ &\leq \|(I - \eta H)\|^t \|x_1 - x_0\| \\ &\leq (1 + \eta\lambda)^t r \|\nabla f_z(x_0)\| \\ &\leq \kappa^t rl. \end{aligned}$$

■

Lemma 33 Assume $E[f(x_t)] - f(x_0) \geq -f_{thres}$ holds, then we can get

$$E[\|\delta_t\|] \leq \left(\frac{2\rho C f_{thres}}{\eta^2 \lambda^2} + \frac{\rho CL(lr)^2}{\eta^2 \lambda^2} + \frac{2\rho l^2 r^2}{\eta \lambda} \right) \kappa^t.$$

Proof

$$\begin{aligned} E[\|\delta_t\|] &= E\left[\left\| \sum_{k=1}^t (I - \eta H)^{t-k} (\nabla g(x_k) - \nabla f(x_k)) \right\|\right] \\ &\leq \sum_{k=1}^t (1 + \eta\lambda)^{t-k} E[\|\nabla g(x_k) - \nabla f(x_k)\|] \\ &\leq \frac{\rho}{2} \sum_{k=1}^t (\kappa)^{t-k} E[\|x_k - x_0\|^2] \\ &\leq \left(\frac{2\rho C f_{thres}}{\eta^2 \lambda^2} + \frac{\rho CL(lr)^2}{\eta^2 \lambda^2} + \frac{2\rho l^2 r^2}{\eta \lambda} \right) \kappa^t. \end{aligned}$$

■

Lemma 34 [Distance Lower Bound] Suppose that expectation of the decrease function value is lower-bounded:

$$E[f(x_t)] - f(x_0) \geq -f_{thres}.$$

Then, the expectation of the distance from the current iteration x_{t+1} to \tilde{x}^0 is bounded as

$$E[\|x_{t+1} - x_0\|^2] \geq \frac{1}{3} \tau r^2 \kappa^{2\frac{t}{\mathcal{K}}(\mathcal{K}-1)}. \quad (19)$$

where $t = \sum_{k=1}^{\mathcal{K}-1} N_k$.

Proof

We know that

$$\begin{aligned}
 E[u_t]^T E[\zeta_t] &= 0; \\
 E[\|u_t^T d_t\|] &> 0 \text{ by Lemma 29;} \\
 E[\|u_t\|^2] &\geq \tau r^2 \kappa^{2t} \text{ by Lemma 30;} \\
 E[\|u_t\|] &\leq r l \kappa^t \text{ by Lemma 32;} \\
 E[\|\delta_t\|] &\leq \left(\frac{2\rho C f_{thres}}{\eta^2 \lambda^2} + \frac{\rho C L (lr)^2}{\eta^2 \lambda^2} + \frac{2\rho l^2 r^2}{\eta \lambda} \right) \kappa^t \text{ by Lemma 33.}
 \end{aligned}$$

$$\begin{aligned}
 E[\|x_{t+1} - x_0\|^2] &\geq E[\|u_t\|^2] - 2\eta E[\|u_t\|] E[\|\delta_t\|] + 2\eta E[u_t]^T d_t + 2\eta E[u_t]^T E[\zeta_t] \\
 &\geq \tau r^2 \kappa^{2t} - 2\eta r l \kappa^t \left(\frac{2\rho C f_{thres}}{\eta^2 \lambda^2} + \frac{\rho C L (lr)^2}{\eta^2 \lambda^2} + \frac{2\rho l^2 r^2}{\eta \lambda} \right) \kappa^t \\
 &\geq \left(\tau r - \left(\frac{4l\rho C f_{thres}}{\eta \lambda^2} + \frac{2\rho C L l^3 r^2}{\eta \lambda^2} + \frac{4\rho l^3 r^2}{\lambda} \right) r \right) \kappa^{2t}.
 \end{aligned}$$

In order to get contradiction on the upper bound and lower bound of $E[\|x_{t+1} - x_0\|^2]$, we will first try to setup parameters for f_{thres} and r for lower bound:

$$\begin{aligned}
 \frac{4\rho l^3 r^2}{\lambda} &\leq \frac{1}{6} \tau r \Rightarrow r \leq \frac{\tau \lambda}{24\rho l^3} \xrightarrow{\lambda \geq \epsilon_h} r \leq \frac{\tau \epsilon_h}{24\rho l^3} \\
 \frac{2\rho C L l^3 r^2}{\eta \lambda^2} &\leq \frac{1}{6} \tau r \Rightarrow r \leq \frac{\eta \tau \lambda^2}{12\rho C L l^3} \xrightarrow{\lambda \geq \epsilon_h} r \leq \frac{\eta \tau \epsilon_h^2}{12\rho C L l^3}, \\
 \frac{4l\rho C f_{thres}}{\eta \lambda^2} &\leq \frac{1}{3} \tau r \Rightarrow f_{thres} \leq \frac{\eta \tau r \lambda^2}{12l\rho C} \xrightarrow{\lambda \geq \epsilon_h} f_{thres} \leq \frac{\eta \tau r \epsilon_h^2}{12l\rho C}.
 \end{aligned}$$

where $\lambda \geq \epsilon_h$ is due to remark 31 Therefore,

$$r \leq \min\left(\frac{\tau}{24\rho l^3}, \frac{\eta \tau}{12\rho C L l^3}\right) \epsilon_h^2 = C_2 \frac{\tau}{12\rho l^3} \epsilon_h^2, \quad (20)$$

$$f_{thres} \leq \frac{\eta \tau r \epsilon_h^2}{12l\rho C}, \quad (21)$$

where $C_2 = \min\left(\frac{1}{2}, \frac{\eta}{C_L}\right)$.

Given above requirements for parameter f_{thres} and r , we obtain the new lower bound:

$$E[\|x_{t+1} - x_0\|^2] \geq E\left[\frac{1}{3} \tau r^2 \kappa^{2t}\right] \quad (22)$$

$$= E\left[\frac{1}{3} \tau r^2 \kappa^{2 \sum_{k=1}^{\mathcal{K}-1} N_k}\right] \quad (23)$$

$$\geq \frac{1}{3} \tau r^2 \kappa^{2 \sum_{k=1}^{\mathcal{K}-1} E[N_k]} \quad (24)$$

$$= \frac{1}{3} \tau r^2 \kappa^{2 \frac{n}{b} (\mathcal{K}-1)} \quad (25)$$

where the last inequality is due to $N_k, k = 1, \dots, \mathcal{K} - 1$ are independent with each other and Jensen inequality. ■

Lemma 35 *If the Hessian matrix at x_0 has a small negative eigenvalue, i.e. $\lambda_{\min}(\nabla f^2(x_0)) \leq -\epsilon_h$ and $\mathcal{K}_{thres} \geq \frac{C_1}{\eta\epsilon_h} \log(\frac{12l}{\tau r \epsilon_h})$, where C_1 is a sufficient large constant, then there exists a state $\mathcal{K} \leq \mathcal{K}_{thres}$ such that expectation of the function value decrease as*

$$f(\tilde{x}^0) - E[f(\tilde{x}^{\mathcal{K}})] \geq f_{thres}.$$

Proof

By Lemma 34, we can see that the distance between x_{t+1} and x_0 is lower bounded by an exponential term in (19)

$$E[\|x_{t+1} - x_0\|^2] \geq \frac{1}{3} \tau r^2 \kappa^{2\frac{n}{b}(\mathcal{K}-1)}.$$

However, in Lemma 27, we also obtain an upper bound for this distance in (15),

$$E[\|x_{t+1} - \tilde{x}^0\|^2] \leq 4\mathcal{K}Cf_{thres} + 2\mathcal{K}CL(lr)^2 + 4(lr)^2 + 2(l\eta)^2$$

which is a linear function in terms of iteration \mathcal{K} .

First, let

$$4\mathcal{K}Cf_{thres} + 2\mathcal{K}CL(lr)^2 + 4(lr)^2 + 2(l\eta)^2 = 0 \quad (26)$$

Put all constrains (20), (21) and $\tau \leq l^2$ into equality (26), we get a new linear function in terms of \mathcal{K} :

$$\left(\frac{\eta^2}{36\rho^2CL} + \frac{\eta^2}{72\rho^2CL^2}\right)\epsilon_h^4\mathcal{K} + 4(lr)^2 + 2(l\eta)^2 = 0 \quad (27)$$

Then based on $\epsilon_h^4 \leq 1$, we get :

$$\left(\frac{\eta^2}{36\rho^2CL} + \frac{\eta^2}{72\rho^2CL^2}\right)\mathcal{K} + 4(lr)^2 + 2(l\eta)^2 = 0 \quad (28)$$

The point of intersection of

$$y = \left(\frac{\eta^2}{36\rho^2CL} + \frac{\eta^2}{72\rho^2CL^2}\right)\mathcal{K} + 4(lr)^2 + 2(l\eta)^2 \quad \& \quad y = \frac{1}{3} \tau r^2 \kappa^{2\frac{n}{b}(\mathcal{K}-1)}$$

is larger than the point of intersection of

$$y = 4\mathcal{K}Cf_{thres} + 2\mathcal{K}CL(lr)^2 + 4(lr)^2 + 2(l\eta)^2 \quad \& \quad y = \frac{1}{3} \tau r^2 \kappa^{2\frac{n}{b}(\mathcal{K}-1)}$$

Therefore, we only need to find the point of intersection \mathcal{K}_{point} of

$$y = \left(\frac{\eta^2}{36\rho^2CL} + \frac{\eta^2}{72\rho^2CL^2}\right)\mathcal{K} + 4(lr)^2 + 2(l\eta)^2 = 0 \quad \& \quad y = \frac{1}{3} \tau r^2 \kappa^{2\frac{n}{b}(\mathcal{K}-1)}$$

and let $\mathcal{K}_{thresh} \geq \mathcal{K}_{point}$.

Let

$$f(\mathcal{K}) = \frac{1}{3} \tau r^2 (1 + \eta\epsilon_h)^{2\frac{n}{b}(\mathcal{K}-1)} - \left(\frac{\eta^2}{36\rho^2CL} + \frac{\eta^2}{72\rho^2CL^2}\right)\mathcal{K} - 4(lr)^2 - 2(l\eta)^2$$

Then we calculate the gradient of $f(\mathcal{K})$ and let it be 0:

$$f'(\mathcal{K}) = \frac{2}{3} \frac{n}{b} \tau r^2 (1 + \eta \epsilon_h)^{2\frac{n}{b}(\mathcal{K}-1)} \log((1 + \eta \epsilon_h)) - \left(\frac{\eta^2}{36\rho^2 CL} + \frac{\eta^2}{72\rho^2 CL^2} \right) = 0$$

$$\begin{aligned} \mathcal{K}^* &= \frac{b}{2n} \frac{\log\left(\frac{3b}{2n\tau r^2 \log((1+\eta\epsilon_h))} \left(\frac{\eta^2}{36\rho^2 CL} + \frac{\eta^2}{72\rho^2 CL^2}\right)\right)}{\log(1 + \eta \epsilon_h)} + 1 \\ &\leq \frac{b}{2n\eta\epsilon_h} \log\left(\frac{3b}{2n\tau r^2 \eta \epsilon_h} \left(\frac{\eta^2}{36\rho^2 CL} + \frac{\eta^2}{72\rho^2 CL^2}\right)\right) + 1 \end{aligned}$$

here we use $\log(1 + a) \geq a$ if $a \in (-1, 1]$.

Based on property of function $f(\mathcal{K})$, we know :

$$\begin{aligned} \mathcal{K}_{point} &\leq 2\mathcal{K}^* + \frac{4(lr)^2 + 2(l\eta)^2}{\left(\frac{\eta^2}{36\rho^2 CL} + \frac{\eta^2}{72\rho^2 CL^2}\right)} \\ &= \frac{b}{n\eta\epsilon_h} \log\left(\frac{3b}{2n\tau r^2 \eta \epsilon_h} \left(\frac{\eta^2}{36\rho^2 CL} + \frac{\eta^2}{72\rho^2 CL^2}\right)\right) + \frac{4(lr)^2 + 2(l\eta)^2}{\left(\frac{\eta^2}{36\rho^2 CL} + \frac{\eta^2}{72\rho^2 CL^2}\right)} + 2 \\ &= \frac{b}{n\eta\epsilon_h} \left(\log\left(\frac{1}{\epsilon_h^5}\right) + \log\left(\frac{3 * 144\rho^2 l^6 b}{2nC_2^2 \tau^3 \eta} \left(\frac{\eta^2}{36\rho^2 CL} + \frac{\eta^2}{72\rho^2 CL^2}\right)\right)\right) + \frac{4(lr)^2 + 2(l\eta)^2}{\left(\frac{4\eta}{CL\rho^2} + \frac{2\eta^2}{144CL^2\rho^2}\right)} + 2 \\ &= \frac{b}{n\eta\epsilon_h} \log\left(\frac{1}{\epsilon_h^5}\right) \left(1 + \frac{1}{\log\left(\frac{1}{\epsilon_h^5}\right)} \log\left(\frac{3 * 144\rho^2 l^6 b}{2nC_2^2 \tau^3 \eta} \left(\frac{\eta^2}{36\rho^2 CL} + \frac{\eta^2}{72\rho^2 CL^2}\right)\right)\right) + \frac{\epsilon_h}{\log\left(\frac{1}{\epsilon_h^5}\right)} \left(\frac{4(lr)^2 + 2(l\eta)^2}{\left(\frac{\eta^2}{36\rho^2 CL} + \frac{\eta^2}{72\rho^2 CL^2}\right)} + 2\right) \\ &\leq \frac{b}{n\eta\epsilon_h} \log\left(\frac{1}{\epsilon_h^5}\right) \left(1 + \frac{1}{\log\left(\frac{1}{(0.1)^5}\right)} \log\left(\frac{3 * 144\rho^2 l^6 b}{2nC_2^2 \tau^3 \eta} \left(\frac{\eta^2}{36\rho^2 CL} + \frac{\eta^2}{72\rho^2 CL^2}\right)\right)\right) + \frac{1}{\log\left(\frac{1}{(0.1)^5}\right)} \left(\frac{4(lr)^2 + 2(l\eta)^2}{\left(\frac{4\eta}{CL\rho^2} + \frac{2\eta^2}{144CL^2\rho^2}\right)} + 2\right) \\ &\leq \frac{b}{n\eta\epsilon_h} \log\left(\frac{1}{\epsilon_h^5}\right) \left(1 + \frac{1}{\log\left(\frac{1}{(0.1)^5}\right)} \log\left(\frac{3 * 144\rho^2 l^6 b}{2nC_2^2 \tau^3 \eta} \left(\frac{\eta^2}{36\rho^2 CL} + \frac{\eta^2}{72\rho^2 CL^2}\right)\right)\right) \\ &\quad + \frac{1}{\log\left(\frac{1}{(0.1)^5}\right)} \left(\frac{4(l)^2 C_2 \frac{\tau}{12\rho l^3} + 2(l\eta)^2}{\left(\frac{\eta^2}{36\rho^2 CL} + \frac{\eta^2}{72\rho^2 CL^2}\right)} + 2\right) \\ &\leq C_1 \frac{b}{n\eta\epsilon_h} \log\left(\frac{1}{\epsilon_h^5}\right) \end{aligned}$$

where $C_1 \geq \left(1 + \frac{1}{\log\left(\frac{1}{(0.1)^5}\right)} \log\left(\frac{3 * 144\rho^2 l^6 b}{2nC_2^2 \tau^3 \eta} \left(\frac{\eta^2}{36\rho^2 CL} + \frac{\eta^2}{72\rho^2 CL^2}\right)\right)\right) + \frac{1}{\log\left(\frac{1}{(0.1)^5}\right)} \left(\frac{4(l)^2 C_2 \frac{\tau}{12\rho l^3} + 2(l\eta)^2}{\left(\frac{4\eta}{CL\rho^2} + \frac{2\eta^2}{144CL^2\rho^2}\right)} + 2\right)$

In summary, the lower bound will be eventually larger than the upper bound with the increase of epoch \mathbb{K} and let $\mathcal{K}_{thres} \geq \frac{C_1}{\eta\epsilon_h} \frac{n}{b} \log\left(\frac{1}{\epsilon_h}\right)$, where C_1 is a sufficient large constant and independent with ϵ_h . The contradiction is introduced and the assumption about decrease of function value is broken. ■

Proof of Convergence In order to cooperate with constraints derived in previous cases, g_{thres} should be carefully selected. We argue that constants γ and C_1 exist such that

$$\frac{10l^2\gamma^2}{L\delta}\left(\frac{b}{n}\right)^{\frac{1}{3}} \leq \frac{n}{b} \frac{\eta^2\epsilon_h^3\tau r}{C_1 12l\rho C} \log^{-1}\left(\frac{1}{\epsilon_h}\right) \leq \frac{\gamma}{5L}\left(\frac{n}{b}\right)^{\frac{1}{3}}\epsilon_g^2,$$

where γ is a small constant and C_1 is a large constant.

With above argument about the existence of γ, C_1 , let $g_{thres} = \frac{\eta^2\epsilon_h^3\tau r}{C_1 12l\rho C} \log^{-1}\left(\frac{12l}{\tau r\epsilon_h}\right)$ and we are ready to prove the main theorem under probabilistic setting.

We define event A_t as

$$A_t := \{\|\nabla f(\tilde{x}^t)\| \geq \epsilon_g \text{ or } \lambda_{min}(\nabla^2 f(\tilde{x}^t)) \leq -\epsilon_h\}.$$

Let R be a random variable represented the ratio of second-order stationary points visited at the end of each epoch in past T epochs by our algorithm. Hence: $R = \frac{1}{T} \sum_{t=1}^T \mathbf{I}(A_t^c)$, where $\mathbf{I}(\cdot)$ is an indicator function. Further, let P_t be the probability of event A_t and $1 - P_t$ be the probability of its complement A_t^c . Our goal will be

$$E(R) = \frac{1}{T} \sum_{t=1}^T (1 - P_t)$$

in high probability, which means:

$$E(R) = \frac{1}{T} \sum_{t=1}^T (1 - P_t) \geq 1 - \delta,$$

or

$$\frac{1}{T} \sum_{t=1}^T P_t \leq \delta.$$

Estimating the probabilities P_t for $t \in \{1, \dots, T\}$ are very difficult. However, we can bound them together. Our algorithm obtains the guaranteed function value decrease per epoch in large gradient and large negative curvature regimes:

$$E[f(\tilde{x}^t) - f(\tilde{x}^{t-1})|A_t] \leq -g_{thres},$$

and the increase of function value around second-order stationary points is controlled by our choice of parameters:

$$E[f(\tilde{x}^t) - f(\tilde{x}^{t-1})|A_t^c] \leq \delta g_{thres}/2.$$

Then we can obtain expected change of function values:

$$E[f(\tilde{x}^t) - f(\tilde{x}^{t-1})] \leq \delta(g_{thres}/2)(1 - P_t) - g_{thres}P_t.$$

Summing the above inequality over the T and reorganizing, we obtain:

$$\frac{1}{T} \sum_{t=1}^T P_t \leq \frac{f(x_0) - f^*}{T g_{thres}} + \frac{\delta}{2} \leq \delta.$$

Therefore,

$$T = \frac{2(f(x_0) - f^*)}{\delta g_{thres}} = \frac{b}{n} \frac{288CC_1\rho^2 l^4 (f(x_0) - f^*)}{C_2\delta\eta^2\tau^2\epsilon_h^5} \log\left(\frac{1}{\epsilon_h}\right) = \frac{b}{n} \frac{288CC_1 l^4 (f(x_0) - f^*)}{C_2\delta\eta^2\tau^2\epsilon^2} \log\left(\frac{1}{\sqrt{\rho}\epsilon^{\frac{2}{5}}}\right).$$

C.6 Proof of Computational Complexity

Considering constants C, C_1, C_2 and γ in Theorem 3.1 are independent of ϵ , the convergence rate will be $E[\sum_{k=1}^T N_k] = \frac{n}{b}T = \tilde{O}(\epsilon^{-2} \log(1/\epsilon))$. If we further require $C_4 = \frac{n}{b}$ to be a constant independent with n , then the number of epochs T only depends on $C_4 = \frac{n}{b}$. Therefore, the number of IFO calls can be derived by $E[\sum_{k=1}^T (n + bN_k)] = 2nT = O(n\epsilon^{-2} \log(1/\epsilon))$.

Appendix D. Proofs for the proposed general framework

As the same situation in Neon and Neon2, generic framework also depends on how to check the ϵ_g -first-order condition (Line 3). In practice, we can use some approximation approaches to check the ϵ_g -first-order condition. For practical consideration, we can make sample size $|S|$ large enough and use $\nabla f_S(x_{t-1}^k)$ to check ϵ_g -first-order condition. When we say sample size large enough, it means that $\|\nabla f_S(x_{t-1}^k) - \nabla f(x_{t-1}^k)\| \leq \epsilon/2$ with high probability $1 - \delta$, hence $\|\nabla f_S(x_{t-1}^k)\| \leq \epsilon/2$ can guarantee that $\|\nabla f(x_{t-1}^k)\| \leq \epsilon$ with high chance. We say the ϵ_g -first-order stationary point is found and the algorithm is ready for SGD jump step. The sample size $|S|$ can be determined by the following lemma which was first established in (Ghadimi et al., 2016):

Lemma 36 *Suppose function f is gradient-bounded. Let $\nabla f_S(x) = \frac{1}{|S|} \sum_{z \in S} \nabla f_z(x)$, for any $\epsilon, \delta \in (0, 1)$, $x \in \mathbb{R}^d$, when $|S| \geq \frac{2l^2(1+\log(1/\delta))}{\epsilon^2}$, we have $Pr(\|\nabla f_S(x) - \nabla f(x)\| \leq \epsilon) \geq 1 - \delta$.*

D.1 Proof of Theorem 4.3

Lemma 4.1 guarantees that the decrease of function value per epoch in expectation around strict saddle points is D_e . The assumption about algorithm \mathcal{A} in Theorem 4.2 makes sure that \mathcal{A} will drop function value in $D_{\mathcal{A}(\epsilon_g)}$ per epoch in expectation when $\|\nabla f(x)\| > \epsilon_g$ and won't increase function value too much in expectation when $\|\nabla f(x)\| \leq \epsilon_g$ and $\lambda_{\min}(\nabla^2 f(x)) \leq \epsilon_h$. Then let $g_{thres} = \min(D_e, D_{\mathcal{A}(\epsilon_g)})$ and follow previous argument for main Theorem, we can obtain the desired result.

Appendix E. A concrete case for algorithm \mathcal{A}

Let algorithm \mathcal{A} be one epoch of SCSG with batch size B_1 and b_1 , then by Theorem 3.1, we can obtain that

$$E[\|\nabla f(y)\|^2] \leq \frac{5b_1}{\eta B_1} E[f(x) - E(y)] + \frac{6\mathbf{I}(B_1 < n)}{B_1} l^2$$

where $\mathbf{I}(\cdot)$ is an indicator function.

When $\|\nabla f(y)\| > \epsilon_g$,

$$\begin{aligned} E[f(x) - E(y)] &\geq \frac{\eta B_1}{b_1} (\epsilon_g^2 - \frac{6\mathbf{I}(B_1 < n)}{B_1} l^2) \\ &\geq \frac{\eta B_1}{2b_1} \epsilon_g^2 \end{aligned}$$

Algorithm 5 SCSG-epoch

Require: x, η, B_1, b_1

 Randomly pick $I_B \in \{1, \dots, n\}$ where $|I_B| = B_1$
 $\tilde{\mu} = \nabla f_{I_B}(x)$

 Generate $N \sim \text{Geom}(B_1/b_1 - b_1)$
for $t = 1, 2, \dots, N$ **do**

 Randomly pick $I_b \subset \{1, \dots, n\}$ and update weight, where $|I_b| = b_1$
 $x_t = x_{t-1} - \eta(\nabla f_{I_b}(x_{t-1}) - \nabla f_{I_b}(x) + \tilde{\mu})$
end for

 return $y = x_N$

where $B_1 \geq \frac{12l^2}{\epsilon_g^2}$. Therefore, $D_{\mathcal{A}(\epsilon_g)} = \frac{\eta B_1}{2b_1} \epsilon_g^2$.

When $\|\nabla f(y)\| \leq \epsilon_g$,

$$\begin{aligned} E(f(y) - E(x)) &\leq \frac{\eta B_1}{b_1} \left(\frac{6\mathbf{I}(B_1 < n)}{B_1} l^2 \right) \\ &\leq \frac{\eta}{2b_1} l^2. \end{aligned}$$

Then, the expected increase of function value is $\frac{\eta}{2b_1} l^2$. Let

$$\frac{\eta}{2b_1} l^2 \leq \min(D_e, D_{\mathcal{A}(\epsilon_g)}),$$

$$b_1 \geq \frac{\eta l^2}{2} \max\left(\frac{1}{D_e}, \frac{1}{D_{\mathcal{A}(\epsilon_g)}}\right).$$

Therefore, when $b_1 \geq \frac{\eta l^2}{2} \max(\frac{1}{D_e}, \frac{1}{D_{\mathcal{A}(\epsilon_g)}})$ and $B_1 \geq \max(\frac{12l^2}{\epsilon_g^2}, b_1)$, SCSG-epoch satisfies the assumption of algorithm \mathcal{A} .

Appendix F. The anisotropic noise in SGD

In this section, we intend to justify the CNC-assumption. In non-convex optimization, the updating formula for SGD is:

$$x_{t+1} = x_t - r \nabla f_z(x_t),$$

where r is the stepsize, z is randomly sampled from $\{1, 2, \dots, n\}$.

Then we know the covariance matrix of stochastic gradient $\nabla f_z(x)$:

$$\begin{aligned}
 \text{Var}(\nabla f_z(x)) &= \frac{1}{n} \sum_{z=1}^n (\nabla f_z(x) - \nabla f(x))(\nabla f_z(x) - \nabla f(x))^T & (29) \\
 &= \frac{1}{n} \sum_{z=1}^n \nabla f_z(x)(\nabla f_z(x))^T - \nabla f(x)(\nabla f(x))^T \\
 &\Downarrow \\
 &\text{around saddle points} \implies \|\nabla f(x)\| \leq \epsilon \\
 &\Downarrow \\
 &\approx \frac{1}{n} \sum_{z=1}^n \nabla f_z(x)(\nabla f_z(x))^T \\
 &= F_E(x),
 \end{aligned}$$

where $F_E(x)$ is empirical fisher information matrix.

Lemma 37 Assume $P(z|x) \propto \exp^{-f_z(x)}$, then

$$E_{P(z|x)}[\nabla^2 \log(P(z|x))] = -F,$$

where $F = E_{P(z|x)}[\nabla f_z(x)\nabla f_z(x)^T]$ is Fisher information matrix.

Proof

$$\begin{aligned}
 \nabla^2 \log(P(z|x)) &= \frac{\nabla^2 P(z|x)P(z|x) - \nabla P(z|x)\nabla P(z|x)^T}{P(z|x)P(z|x)} \\
 &= \frac{\nabla^2 P(z|x)P(z|x)}{P(z|x)P(z|x)^T} - \frac{\nabla P(z|x)\nabla P(z|x)^T}{P(z|x)P(z|x)} \\
 &= \frac{\nabla^2 P(z|x)}{P(z|x)} - \frac{\nabla P(z|x)}{P(z|x)} \left(\frac{\nabla P(z|x)}{P(z|x)} \right)^T.
 \end{aligned}$$

Therefore:

$$\begin{aligned}
 &E_{P(z|x)}[\nabla^2 \log(P(z|x))] \\
 &= E_{P(z|x)}\left[\frac{\nabla^2 P(z|x)}{P(z|x)}\right] - E_{P(z|x)}\left[\frac{\nabla P(z|x)}{P(z|x)} \left(\frac{\nabla P(z|x)}{P(z|x)}\right)^T\right] \\
 &= -E_{P(z|x)}[\nabla \log(P(z|x))(\nabla \log(P(z|x)))^T] \\
 &= -E_{P(z|x)}[\nabla f_z(x)f_z(x)^T] \\
 &= -F
 \end{aligned}$$

where F is Fisher information matrix. ■

Around saddle points, the variance-covariance matrix of the stochastic gradient $\nabla f_z(x)$ is approximately equal to the empirical Fisher's information matrix (see Appendix). In

practice, under the assumptions that the sample size n is large enough and the current x is not too far away from the ground truth parameter, Fisher's information matrix $E_{P(z|x)}[\nabla^2 \log(P(z|x))]$ approximately equals to the Hessian matrix H of $f(\cdot)$ at x . Thus, the intrinsic noise in SGD is naturally embedded into Hessian information. This explains the anisotropic behavior of the noise in SGD.